14. MINERALOGY AND INORGANIC GEOCHEMISTRY OF SEDIMENTS FROM THE MOUTH OF THE GULF OF CALIFORNIA[1]

Victor B. Kurnosov, Far-East Geological Institute, USSR Academy of Sciences, Vladivostok, USSR
Ivar O. Murdmaa, Vera Kazakova, and Alla Shevchenko, P. P. Shirshov Institute of Oceanology,
USSR Academy of Sciences, Moscow, USSR
and
Vladlena Mikhina, Polytechnical Institute, Moscow, USSR

INTRODUCTION

During Leg 65, 15 holes were drilled at four sites located on young crust in the mouth of the Gulf of California. Quaternary to upper Pliocene hemipelagic sediments above and interlayered within the young basaltic basement were cored. The influence of hot lava, high temperature gradients, and hydrothermal activity on the mineralogy and geochemistry of the terrigenous sediments near contacts with basalts might therefore be expected.

The purpose of the present study was to determine the mineralogy and inorganic geochemistry of these sediments and to analyze the nature and extent of low temperature alteration. To this end we studied the mineralogy and inorganic geochemistry of 75 sediment samples, including those immediately overlying uppermost basalts and those from layers alternating with basalts within the basement. We separated three size fractions— <2 μm (clay), 2–20 μm (intermediate), and >20 μm (coarse)—and applied the following mineralogical determinations: x-ray diffraction (XRD), infrared spectroscopy, transmission and scanning electron microscopy, and optical microscopy (for coarse fractions, using thin sections and smear slides). We calculated the percentages of clay minerals using Biscaye's (1964) method, and used routine wet chemical analyses to determine bulk composition and quantitative spectral analyses for trace elements.

SITE 482

Site 482 was located 12 km east of the East Pacific Rise and 15 km south of the Tamayo Fracture Zone. The age of the basement is about 0.5 m.y. The thickness of upper Quaternary sediments above the basalt is 140 meters; these are olive gray hemipelagic clay or silty clay, with admixtures of nannofossils, foraminifers, radiolarians, and diatoms. Sedimentation rates vary from 343 to 548 m/m.y. The temperature at the sediment/basalt contact was 90°C in Hole 482C, and the geothermal gradient calculated for the site equaled 67° per 100 meters. Notwithstanding the high temperature, the basalts are no more altered than most of the oceanic tholeiites.

We studied sediments from five of the holes drilled at Site 482: Holes A, B, C, D, and F. Three samples are from sediments interlayered within basalts: Hole 482B-19-1, 31–33 cm and 47–49 cm, and Hole 482D-9-1, 3–7 cm. Several samples were taken from sediments immediately overlying basement. Sample 482B-10-7, 4–6 cm represents a contact with basalt, Sample 482B-10-6, 139–141 cm was taken 15 cm above the contact. Sample 482F-4-3, 100–102 cm is from the sediment/basalt contact. Sample 482C-9-1, 12–14 cm is from 40 cm above the contact. The lowermost sediment sample from Hole 482D (Core 7, Section 3, 145–147 cm) was recovered less than 4.5 meters above the first basalt sampled.

Mineralogy

It is clear from smear-slide and thin section analysis that the sediments at Site 482 are of terrigenous origin with an admixture of more or less abundant biogenic calcite (foraminifers, nannofossils, and unidentified fragments), minor biogenic opal (radiolarian and diatom fragments plus rare spicules), and organic matter (plant debris, sapropels), with variable amounts of the following authigenic minerals: pyrite, glauconite, carbonates of the dolomite-ankerite-siderite group, barite, and zeolite (clinoptilolite).

The terrigenous matter is composed of clay minerals and clastic grains of quartz, feldspar, (mainly plagioclase), mica, and heavy minerals such as epidote, zircon, amphiboles, and apatite. The clastic minerals are concentrated in the silt and fine sand fractions, where quartz and feldspars predominate. The relative abundance of clastic minerals therefore varies with the average grain size.

Pyrite occurs throughout the sediment section and commonly predominates over the other authigenic minerals. As indicated visually in smear slides, it amounts up to 1 to 3% total sediment composition, but tends to increase with depth. The common forms are microspherules, 2 to 20 μm in diameter or less, which occur separately in the clay matrix or concentrated on organic matter fragments, foraminifer tests, etc. Along with spherules we observed irregular aggregates of pyrite and pyrite pseudomorphs after plant debris. Cubic crystals are rare.

The authigenic carbonates seem to vary widely in composition, as indicated by differences in color and re-

fractive index. Yellowish or reddish brown grains with high refractive indices are likely those of ferroan dolomite (ankerite) or siderite, whereas light yellow or colorless crystals probably represent dolomite. The carbonates are unevenly distributed in the section. The first rare ankerite(?) crystals were noted in the uppermost sample, Sample 482A-1-1, 130–133 cm (1.3 m sub-bottom). Downward in different holes, mineral abundance varies from zero or traces to 1 to 2% of total sediment composition.

Sample 482C-8-1, 106–108 cm (131 m sub-bottom) is composed almost totally of fine-grained, rhombohedral ankerite(?) crystals, 5–7 μm in diameter, with both refractive indices of all grains in thin section higher than that of Canadian balsam (1.54). The x-ray diffraction pattern of the 2–20 μm fraction showed almost pure dolomite, but the high refractive index indicates that it is ferroan. The sample also contains subordinant amounts of spheroidal pyrite, elongated organic particles (plant debris?), and an admixture (1–2%) of clastic quartz and clay minerals.

Relatively abundant authigenic carbonates (of about 3%) were observed in a smear slide of Sample 482C-9-1, 12–14 cm (132.12 m sub-bottom, 40 cm above the basalt), where rhombohedral crystals and microdruses as large as 30 μm occur. The carbonates are also common in samples higher above the basement: Sample 482C-7-6, 25–27 cm (128 m sub-bottom), Sample 482D-1-1, 120–123 cm (77 m sub-bottom), Sample 482D-4-2, 135–137 cm (103 m sub-bottom), and Sample 482D-5-2, 61–63 cm (111.6 m sub-bottom), and in a sample from sediments interbedded within basalts: Sample 482B-19-1, 47–49 cm (193.5 m sub-bottom).

Zeolite (clinoptilolite) crystals, commonly less than 20 μm across, occur sporadically in the upper portion of the section and disappear below 100 to 125 meters sub-bottom, where the present temperature is higher than 60°C. In our set of samples the zeolite is most abundant in sediments from Hole 482A, Cores 1 and 3.

Barite was observed in several thin sections and in smear slides from the lower part of the sediment section, particularly in sediments immediately overlying basalt (Samples 482B-10-7, 4–6 cm and 482C-9-1, 12–14 cm) or intercalated within basalts (Sample 482B-19-1, 47–49 cm), but also in Samples 482D-5-2, 60–63 cm and 482F-3-4, 88–90 cm) (111.6 m and 128 m sub-bottom). The mineral occurs as spherulitic aggregates, 0.3 to 1 mm in diameter, of platy colorless crystals, which show low birefringence, a refractive index higher than 1.54, and positive elongation. The crystals contain numerous inclusions of surrounding sediment particles and are obviously of authigenic origin.

X-ray diffraction studies, in general, confirmed and refined the identifications made by smear-slide and thin-section analysis. In particular, these studies demonstrated the presence of smectites (17 Å minerals), mica, mixed-layer illite–montmorillonite (+mica), chlorite, kaolinite, mixed-layer chlorite-montmorillonite (swelling chlorite), quartz, feldspars, clinoptilolite, calcite, dolomite, an amorphous phase, and pyrite.

In the clay fraction (<2 μm) (Table 1) smectite predominates throughout the section, showing rather irregular variations between 60 and 88 vol.%. The greater values tend to occur in the lower parts of the sediment section—below 100 meters—in Holes 482B, D, and F; but in two samples in Hole 482C, 131 to 132 meters subbottom, we detected low percentages of the mineral. Smectites are absent in the clay fraction immediately overlying basalts and interbedded within basalts in Hole 482D (samples from 133 m and 141.5 m sub-bottom).

The smectite d-spacing ranges from 12.2 to 12.6 Å and increases to values of 16.8 to 17 Å when the samples are treated with glycol. The ratio between the shoulder heights of the 17 Å peak, which we propose to name coefficient z, and which characterizes the peak asymmetry, averages 0.6. In the crystal structure of the smectite a minor number of mica layers may exist. The smectites display a dioctahedral structure. Treatment with 10% HCl indicates that they comprise both aluminous and ferric montmorillonite (Table 2). Low Fe_2O_3 content in samples rich in smectite (Table 3) confirm the presence of Al-montmorillonite. In the sediments just above basalts the Al-montmorillonite predominates over the ferric variety, but in layers intercalated with basalts the two varieties occur in almost equal quantities (Table 2).

Mica and chlorite (the latter detected with kaolinite) occur in minor amounts in the clay fraction. The mica has a dioctahedral structure and is rich in aluminum and ferric iron. Chlorite is trioctahedral with a stable defect structure and tends to be ferro-magnesian in composition. Kaolinite is clearly recognizable on the diffraction diagrams only after treatment with hot 10% HCl (Table 2). The kaolinite was generally recognized both in unaltered sediments and in sediments which made contact with basalts or were intercalated within basalts. However, in Hole 482D near the sediment/basalt contact (Sample 482D-7-3, 146–147 cm) and in sediments intercalated within basalts (Sample 482D-9-1, 3–7 cm), kaolinite is absent and the clay fraction is composed of swelling chlorite (Table 1) and a mixed-layer illite-montmorillonite containing 20 to 30% mica. The latter mineral is characterized by a peak between 10.73 and 10.94 Å on the diffraction diagrams for dry samples. When the samples are treated with glycol, the peak shifts to 9.91–9.93 Å and an additional peak appears at 11–12 Å. After heating at 550°C for one hour, the peak shifts to 10.0–10.4 Å. The mineral is insoluble in hot 10% HCl and its morphology is shown on Plate 1, Figure 3, and Plate 2, Figure 2.

The swelling chlorite contains minor amounts of montmorillonite in its structure. The diffraction diagrams for dry samples show peaks at 14.16 Å, 7.09 Å, 4.70 Å, and 3.53 Å (Sample 482D-7-3, 146–147 cm). After treatment with glycol, the basal reflection shifts to 14.25 Å. After heating, the entire series of peaks disappeared except for a single peak at 13.59 Å. The mineral is soluble in hot 10% HCl.

Clinoptilolite was found by X-ray diffraction only in the upper part of the sediment section cored at Site 482.

It disappears below 124 meters (14 m above basement) in Holes A and B and below 100 meters (33–38 m above basement) in Hole D.

Other minerals occur in the clay fraction, but usually only in trace amounts. In one sample, however (Sample 482C-8-1, 106–108 cm) we observed abundant dolomite (in thin section it resembles ankerite), and several samples from the lowermost portions of the section contain much quartz (Table 1). In Sample 482A-5-7, 23–26 cm we detected traces of actinolite.

Except for clinoptilolite and quartz the dominant minerals are almost equally distributed throughout the sediment section in Holes A, B, and F, including the sediments immediately overlying or inside the basement. Sediments from 129 to 132 meters sub-bottom in Hole C contain in the clay fraction less smectite (35–69%) and more mica (23–50%) than those from the same depth in other holes. The clay fraction of those sediments in contact with basalts and from layers intercalated within basalts in Hole D is composed of unusual clay minerals—swelling chlorite and mixed-layer illite–montmorillonite (+ mica) likely of hydrothermal origin. Smectites near the basalts in all holes display "authigenic" features on SEM photographs.

The intermediate and coarse fractions (2–20 μm and >20 μm, respectively) are markedly enriched in quartz and feldspars in comparison with the clay fraction. In several samples the mica content is also enriched in the coarse fraction (Table 1), but commonly the compositions of the clay minerals in the two fractions are quite similar. The two lowermost samples from Hole 482D, taken just above and inside the basement, for example, contain in the fraction ranging from 2–20 μm, 87 and 90% mixed-layer illite–montmorillonite (+ mica) with 13 and 10% swelling chlorite, as does the clay fraction of the same samples. Interestingly, a coarse sample from just above the basement in Hole 482C (Core 8, Section 1, 106–108 cm) is almost wholly composed of dolomite (ankerite) with a minor admixture of clay minerals and quartz.

On the diffraction diagrams for dry, coarse fractions, peaks at 12.2–12.6 Å and 13.8–14 Å are easily recognizable. Treatments with glycol, with hot 10% HCl, and with heat (at 550°C) indicate that the 13.8–14 Å peak belongs partly to chlorite, but mainly to smectite. The latter is ferric montmorillonite, soluble in hot 10% HCl (Table 2). Therefore, the coarse fractions contain a variety of Fe-montmorillonite with a peak at 13.8–14 Å, which we have not observed in the clay fraction. The swelling chlorite in coarse fractions of the above-mentioned two samples from Hole 482D contains less smectite than the swelling chlorite in clay fractions.

We also studied the mineralogy of the coarse (>20 μm) fraction in 10 samples of Site 482 sediments using the immersion method (Table 3). Heavy-mineral content in these samples ranges from traces to 2.2%. It is composed of 59 to 100% authigenic pyrite. In six samples we found barite (0.4 to 34.3% of the heavy minerals) in platy crystals and angular fragments containing abundant inclusions of clay and pyrite, likely indicative of authigenic origin of the mineral. Barite is common only below 128 meters sub-bottom. Heavy minerals of terrigenous origin are represented by epidote and zircon with minor hornblende, clinopyroxene, apatite, rutile, anatase, corundum, chlorite, and sphene.

The light fraction consists largely of quartz and feldspar which are present in roughly equal amounts. Most of the feldspars show refraction indexes less than 1.54, and are thus sodium plagioclase (albite–oligoclase) and potassium feldspars. In three samples we found gypsum, and in the two uppermost samples, zeolite.

Geochemistry

We determined bulk composition both for bulk sediments and for two size fractions: clay and intermediate (Table 4). Ten samples were analyzed from Site 482, but in only six of them was the amount sufficient to analyze both fractions. The set includes three samples from immediately overlying basement and one from sediments intercalated within basalts. Two samples from Hole 482D, Cores 7 and 9 (Table 4) contain hydrothermal(?) mixed-layer illite–montmorillonite (+ mica) and swelling chlorite; two samples from the same hole (Cores 1 and 5) represent sediments with authigenic carbonates.

The chemical composition of the sediments is uniform, close to that of common hemipelagic mud, almost irrespective of distance from basaltic basement. SiO_2 content in bulk samples ranges from 53 to 58% (Table 4), as in common hemipelagic mud. The silica to alumina ratio (SiO_2/Al_2O_3) in most samples is close to that of average clay (3.5), or somewhat higher (up to 3.8), likely as a result of high terrigenous quartz content. In a sample taken just above basalt (Sample 482F-4-3, 100–102 cm) we detected the lowest value of the ratio (3.2). The sample contains less quartz than others, and the smectite content is high.

Silica is apparently concentrated in the intermediate fraction (60–65% SiO_2; ratio of SiO_2 to Al_2O_3, 4.2–4.7), where x-ray data show the highest quartz and feldspar content. The clay fraction is relatively low in SiO_2 (51–55%) and rich in Al_2O_3 (up to 20.3% near the sediment/basalt contact in Sample 482D-7-3, 145–147 cm), composed mainly of mixed layer illite–montmorillonite (+ mica), whereas in another sample just above basalt (Sample 482B-10-7, 4–6 cm) the clay fraction is relatively enriched in silica.

Titanium content is consistently low throughout, close to that in common hemipelagic clay. The clay fraction is slightly enriched in titanium as compared with the 2–20 μm fraction. The aluminum to titanium ratio, which is sensitive to the presence of volcaniclastic material (Boström, 1976; Murdmaa et al., 1979, 1980) is similar for bulk samples and fractions, ranging from 19 to 24, the values indicative of terrigenous clay and mud.

Iron content is low both in bulk samples and fractions (Table 3). We have not recognized any noticeable enrichment in iron near the sediment/basalt contact or in the sediments intercalated within basalt. The total iron and Fe_2O_3 are somewhat higher in the intermediate fraction and lower in the clay fraction, the state of oxidation showing an apparent decrease in the latter. In two samples of the clay fraction from Hole D, where

Table 1. Mineralogy of sediment fractions, Site 482 (in percent).

Sample (interval in cm)	Sub-bottom Depth (m)	Lithology	Age	Smectite	Mica	Mixed-layer Illite–Montmorillonite plus Mica	Chlorite	Mixed-layer Chlorite–Montmorillonite	Z	Quartz	Clinoptilolite	Amorphous Phase	Calcite	Feldspar	Dolomite
Clay (<2 μm) sediment fraction															
Hole 482A															
1-1, 130–133	1.3	Unit I silty clay	Upper Quaternary	70	20		10	tr	0.5	tr	c	tr		tr	
3-1, 103–106	16.63			60	25		15	tr	0.4	tr	c	tr		tr	
5-7, 23–26	43.73			70	20		10		0.5	tr	c	tr		tr	
Hole 482B															
2-2, 88–90	55.88	Unit I clay and		75	15		10		0.6	tr	c	tr		tr	
4-1, 130–133	73.80	silty clay		65	25		10		0.4	tr	c	tr		tr	
7-2, 94–96	103.44			75	18		7	tr	0.5	tr	c	tr		tr	
9-3, 123–125	124.23			80	17		5		0.6	tr	c	tr		tr	
9-6, 118–120	128.68			75	17		8		0.6	tr		tr		tr	
10-4, 42–44	134.42			80	14		6		0.6	tr		tr		tr	
10-4, 102–104	135.02			78	15		7		0.6	tr		tr		tr	
10-5, 102–104	136.52			72	20		8	tr	0.6	c		tr		tr	
10-6, 139–141	138.39			76	16		8	tr	0.6	c		tr		tr	
10-7, 4–6[a]	138.54			75	14		11		0.6	c		tr		tr	
19-1, 31–33[b]	193.31	Indurated silty clay		73	22		5		0.5	tr		tr		tr	
19-1, 47–49[b]	193.47	and mudstone		73	18		9		0.5	tr		tr		tr	
Hole 482C															
7-6, 25–27	128.25	Unit I silty clay	Upper Quaternary	69	23		8		0.5	tr		tr		tr	
8-1, 106–108	131.06			50	35		15		0.4	c		tr	tr	tr	c
9-1, 12–14[a]	132.12			35	50		15		0.3	c		tr		tr	
Hole 482D															
1-4, 120–123	77.20	Unit I silty clay	Upper Quaternary	62	24		14	tr	0.4	tr	c	tr		tr	
4-2, 135–137	102.85			88	9		3		0.6	tr		tr		tr	
5-2, 60–63	111.60			85	9		7		0.6	tr		tr		tr	
6-3, 21–23	122.21			70	20		10		0.3	tr		tr		tr	
7-3, 145–147[a]	132.95					94	6			tr		tr		tr	
9-1, 3–7[b]	141.53	Nannofossil-bearing silty clay				93	7			tr		tr		tr	
Hole 482F															
3-4, 88–90	128.38	Unit I silty clay	Upper Quaternary	80	13		7		0.6	tr	tr	tr		tr	
4-2, 38–40	133.88			82	14		4		0.5	tr		tr		tr	
4-3, 46–49	135.46			83	11		6		0.6	tr		tr		tr	
4-3, 100–102[a]	136.00			81	13		6		0.6	tr		tr		tr	
Intermediate (2–20 μm) sediment fraction															
Hole 482A															
1-1, 130–133	1.3	Unit I silty clay	Upper Quaternary	48	43		9	tr	0.7	d	d	tr		d	
3-1, 103–106	16.63			45	44		11	tr	0.6	d	d	tr		d	
5-7, 23–26	43.73			65	28		7	tr	0.6	d	c	c			c
Hole 482B															
2-2, 88–90	55.88	Unit I clay and		81	14		5	tr	0.7	c	c	tr		tr	
4-1, 130–133	73.80	silty clay		63	32		5	tr	0.6	d	c	tr		c	
7-2, 94–96	103.44			70	22		8	tr	0.5	d	c	tr		c	

Sample	Depth (m)	Description	Age												
9-3, 123-125	124.23			87	9		4	tr	0.7	c	c		tr		c
9-6, 118-120	128.68			69	25		6	tr	0.6	d			tr	tr	c
10-4, 42-44	134.42			50	37		13	tr	0.7	d			tr		d
10-4, 102-104	135.02			79	14		7	tr	0.6	c			tr		d
10-5, 102-104	136.52			74	16		10	tr	0.6	d.		c			d
10-6, 139-141	138.39			70	20		10	tr	0.6	d			tr		c
10-7, 4-6[a]	138.54			65	24		11	tr	0.5	d			tr		d
19-1, 31-33[b]	193.31	Indurated silty clay		88	7		5	tr	0.6	d			tr		c
19-1, 47-49[b]	193.47	and mudstone		77	15		8	tr	0.6	d			tr		c

Hole 482C

Sample	Depth (m)	Description	Age												
7-6, 25-27	128.25	Unit I silty clay	Upper Quaternary	64	29		7	tr	0.5	d		c			c
8-1, 106-108	131.06			tr	tr					c			tr		tr	d
9-1, 12-14[a]	132.12			52	40		8	tr	0.3	d			tr	tr	c

Hole 482D

Sample	Depth (m)	Description	Age												
1-4, 120-123	77.20	Unit I silty clay	Upper Quaternary	68	23		9	tr	0.5	c	c		tr		c
4-2, 135-137	102.85			79	14		7	tr	0.6	d			tr		c
5-2, 60-63	111.60			71	22		7	tr	0.5	d			tr		c
6-3, 21-23	122.21			65	27		8		0.3	d			c		c
7-3, 145-147[a]	132.95					87	13			d			tr		c
9-1, 3-7[b]	141.53	Nannofossil-bearing silty clay				90	10			d			tr		c

Hole 482F

Sample	Depth (m)	Description	Age												
3-4, 88-90	128.38	Unit I silty clay	Upper Quaternary	78	16		6	tr	0.6	d	c		tr		d
4-2, 38-40	133.88			63	28		9		0.5	d			tr		c
4-3, 46-49	135.46			74	20		6	tr	0.5	c			tr		c
4-3, 100-102[a]	136.00			72	18		10	tr	0.6	c			tr		c

Coarse (>20 μm) sediment fraction

Hole 482A

Sample	Depth (m)	Description	Age												
3-1, 103-106	16.63	Unit I silty clay	Upper Quaternary	71	23		6	tr	0.7	d	c	c			d

Hole 482B

Sample	Depth (m)	Description	Age												
9-6, 118-120	128.68	Unit I clay and silty clay		75	20		5	tr	0.6	c			tr	tr	c
10-4, 102-104	135.02			70	22		8	tr	0.5	d			tr		c
10-7, 4-6	138.54			75	15		10	tr	0.7	d			c		c

Hole 482C

Sample	Depth (m)	Description	Age												
9-1, 12-14	132.12	Unit I silty clay		54	35		11	tr	0.3	d			tr		c

Hole 482D

Sample	Depth (m)	Description	Age												
5-2, 60-69	111.60	Unit I silty clay		81	12		7	tr	0.4	c		c			c
9-1, 3-7[a]	114.53					95	5			d			tr		c

Hole 482F

Sample	Depth (m)	Description	Age												
3-4, 88-90	128.38	Unit I silty clay		61	29		10	tr	0.6	d	c	d			d
4-3, 100-102[a]	136.00			76	15		9	tr	0.6	d		c			c

[a] Sediments immediately overlying basement.
[b] Sediments intercalated within basalts.
[c] Moderate.
[d] Abundant.
[e] Tr = trace.

Table 2. Results of acid dissolution tests on sediments from Sites 482, 483, 484, and 485.

Sample (interval in cm)	Sub-bottom Depth (m)	Sediments Tested[a]	
		Clay Fraction (< 2 μm)	2–20 μm Fraction
Hole 482A			
5-7, 23–26	43.73	Montmorillonite < Fe-montmorillonite	Montmorillonite < Fe-montmorillonite, kaolinite
Hole 482B			
10-7, 4–6[b]	138.54	Montmorillonite > Fe-montmorillonite, kaolinite	
19-1, 31–33[c]	193.31	Montmorillonite ≈ Fe-montmorillonite, kaolinite	
19-1, 37–49[c]	193.47	Montmorillonite ≈ Fe-montmorillonite, kaolinite	
Hole 482C			
9-1, 12–14[b]	132.12	Montmorillonite > Fe-montmorillonite, kaolinite	
Hole 482D			
5-2, 60–63	111.60	Montmorillonite > Fe-montmorillonite, kaolinite	
9-1, 3–7[c]	141.53	Mixed-layer mineral insoluble, chlorite dissolved, kaolinite absent	
Hole 482F			
4-3, 100–102[b]	136.00	Montmorillonite > Fe-montmorillonite, kaolinite	
Hole 483			
7-5, 90–92[b]	55.40	Montmorillonite > Fe-montmorillonite, kaolinite	Montmorillonite ≈ Fe-montmorillonite, kaolinite
13-3, 50–52[b]	109.00	Montmorillonite > Fe-montmorillonite, kaolinite	Montmorillonite ≪ Fe-montmorillonite, kaolinite
18-2, 55–57[c]	153.05	Montmorillonite ≤ Fe-montmorillonite, kaolinite	Montmorillonite ≪ Fe-montmorillonite
18-4, 63–65[c]	156.13	Montmorillonite ≤ Fe-montmorillonite, kaolinite	
Hole 484A			
6-5, 23–25[b]		Montmorillonite ≤ Fe-montmorillonite, kaolinite	
Hole 485			
1-2, 90–94	2.40	Montmorillonite ≈ Fe-montmorillonite, kaolinite	
Hole 485A			
1-5, 120–124	52.10	Montmorillonite > Fe-montmorillonite, kaolinite	
5-3, 111–115	92.61	Montmorillonite ≈ Fe-montmorillonite, kaolinite	
11-2, 107–111	148.07	Montmorillonite > Fe-montmorillonite, kaolinite	Montmorillonite ≪ Fe-montmorillonite, kaolinite
11-3, 35–37[b]	158.35	Montmorillonite < Fe-montmorillonite, kaolinite	
20,CC[c]	197.02		Montmorillonite ≤ Fe-montmorillonite, kaolinite
26-1, 48–50[c]	226.48	Montmorillonite < Fe-montmorillonite	
28-1, 148–150[c]	236.48	Mixed-layer mineral insoluble	
38-1, 98–100[c]	313.98	Mixed-layer mineral dissolved	

[a] One hour in 10% HCl at 90–100°C.
[b] Sediments immediately overlying basement.
[c] Sediments intercalated within basement.

we detected hydrothermal(?) authigenic clay minerals (mixed-layer illite–montmorillonite (+ mica) and swelling chlorite), FeO even predominates over Fe_2O_3, whereas in other samples the latter is 1.5 to 2.3 times higher than FeO. In the 2–20 μm fraction, the Fe_2O_3 to FeO ratio increases up to 6.2, likely as a result of higher Fe-montmorillonite content.

Manganese commonly shows low values throughout the set of samples analyzed, without any increasing trend toward basalts. We did not notice any evidence of exhalative or hydrothermal Mn precipitation.

Magnesium content does not show any significant variation. It is higher in the clay fraction as a result of concentration in clay minerals, but does not increase in the sediments with mixed-layer illite–montmorillonite (+ mica) and swelling chlorite. Variations in calcium content are likely caused by biogenic calcite.

Sodium and potassium content depend on their association with clay minerals and feldspars, so their distribution is rather irregular. However, we can observe a trend toward increasing K_2O content downhole as well as in the K_2O to Na_2O ratio in the clay fraction. The greatest values of the ratio (3.6–4.4) occur below 110 meters in the clay fraction of samples from the sedi-

ment/basalt contact and from a layer inside basement. Total alkalinity, expressed as $K_2O + Na_2O/Al_2O_3$ ranges from 0.16 to 0.46 without any distinct relation to distance from basalts. It is lower in the clay fraction as a result of higher aluminum content.

Phosphorus content is evenly low throughout the section.

Trace elements in all holes studied at Site 482 show similar distribution patterns (Table 5). In bulk samples the trace elements are rather evenly distributed irrespective of their proximity to basalts, except for boron, which decreases markedly near the sediment/basalt contact and in sediments intercalated within basalts. The latter samples show relatively low Mo and Ni contents as well. Concentrations of all trace elements studied in bulk samples are similar to those in common hemipelagic sediments, for example to those drilled during Legs 56 and 57 in the Japan trench (Murdmaa et al., 1980), although Co and Cu contents are lower and Ni and Zn contents somewhat higher in the sediments from the mouth of the Gulf of California.

In the clay fraction, distribution of most of the trace elements is also rather uniform, no apparent changes occurring either near the sediment/basalt contact or in

Table 3. Mineralogy of the coarse (>20 μm) sediment fraction as determined by the immersion method, Sites 482, 483, 484, and 485.

Sample (interval in cm)	Black opaques	Fe-oxides	Pyrite	Garnet	Horn-blende	Clino-pyroxene	Epidote	Zircon	Apatite	Rutile	Anatase	Corundum	Sphene	Biotite	Barite	Carbonates	Quartz	Feldspar	Mica	Opal (biogenic)	Carbonate (biogenic)	Zeolite	Gypsum	Opal(?)[b]
482B-2-2, 88-90	1	—	80	—	1	—	10	6	1	+	+	—	—	—	1	—	17	24	—	—	—	2	2	7
482B-10-4, 42-44	1	—	78	—	—	—	5	1	1	—	—	—	—	—	14	—	28	20	+	+	—	1	—	9
482C-7-6, 25-27	—	—	79	—	—	—	1	+	—	—	—	—	—	—	19	—	3	4	—	—	1	—	—	—
482C-8-1, 106-108	—	2	95	—	—	+	+	+	—	—	+	+	—	—	+	—	2	—	—	—	—	—	1	—
482D-1-4, 120-123	1	2	76	—	2	—	14	3	2	—	—	—	+	—	—	—	16	23	—	2	—	—	—	10
482D-4-2, 135-137	—	2	93	—	—	+	—	3	+	—	—	1	—	—	—	—	20	16	—	—	2	—	6	6
482D-6-3, 21-23	—	—	100	—	—	—	—	—	—	—	—	—	—	—	—	—	15	16	+	—	—	—	—	4
482D-7-3, 145-147[c]	—	1	96	—	+	—	—	2	1	+	—	—	—	—	—	+	6	5	—	—	—	—	—	—
482F-4-2, 38-40[c]	—	—	84	—	—	—	1	2	+	—	—	—	—	—	12	—	23	35	—	—	—	—	—	3
482F-4-3, 46-49[c]	2	1	59	—	+	—	—	1	2	—	—	+	—	—	34	—	4	6	—	—	—	—	—	—
483-9-2, 60-62	—	—	90	—	3	+	5	1	1	—	—	—	+	—	—	+	27	22	3	2	—	—	—	—
483-12-3, 88-90	—	—	95	—	3	—	—	—	—	—	—	—	—	2	—	—	—	—	—	—	—	—	—	—
483-13-1, 120-122	4	—	61	+	2	—	17	3	3	—	—	—	+	—	—	—	26	40	1	—	—	—	—	6
483B-2-6, 93-97	1	—	72	—	2	—	19	3	2	—	—	—	—	—	+	—	30	39	2	—	—	—	—	3
484A-6-5, 23-25[c]	—	—	93	—	3	—	3	1	+	—	—	—	—	—	—	—	14	13	2	9	1	—	—	2
485A-3-2, 5-9	8	+	60	+	3	—	20	5	2	+	—	—	—	1	—	—	21	27	1	—	—	1	—	3
485A-4-1, 63-66	4	—	58	+	3	—	28	3	4	—	—	—	—	—	—	—	5	9	—	—	—	—	—	—
485A-5-3, 111-115	9	—	48	2	—	3	28	6	3	—	—	—	—	—	—	—	22	19	—	2	—	—	3	3
485A-6-4, 110-114	9	—	70	—	1	—	14	5	—	—	—	—	—	—	—	—	31	45	1	7	—	—	—	8
485A-9-1, 128-132	16	3	52	+	1	2	19	5	1	+	+	—	—	—	+	—	10	10	1	—	—	—	2	—
485A-10-2, 104-107	—	—	71	—	1	+	20	6	2	—	—	—	—	—	—	—	16	14	—	—	—	—	—	10
485A-19-2, 40-42[d]	5	—	63	—	6	—	18	6	1	—	—	—	+	—	—	—	20	11	—	—	2	—	—	4
20,CC[d]	—	—	100	—	—	—	—	—	—	—	—	—	—	—	—	—	20	12	—	—	2	—	1	3
485A-22-2, 24-26[d]	4	—	53	—	2	—	23	3	2	—	—	—	—	—	13	—	18	12	—	—	—	—	—	7
485A-22-4, 33-36[d]	10	—	44	+	—	—	33	6	2	—	—	—	—	1	4	—	26	29	—	—	2	—	—	7
485A-27-1, 46-48[d]	3	—	56	—	4	—	24	3	2	—	—	—	—	—	8	—	—	—	—	—	—	—	—	—
485A-34-1, 33-35[d]	5	1	69	—	+	—	16	3	2	—	—	—	—	—	4	—	20	26	—	—	—	—	—	4
485A-36-1, 61-65[d]	—	—	93	—	—	—	6	1	+	—	—	—	—	—	—	—	9	16	—	—	—	—	—	2

[a] The remainder of the light fraction is composed of clay pellets, rock fragments, and altered minerals.
[b] "Opal?" is an unidentified isotropic colorless mineral with a low refraction index, of authigenic appearance.
[c] Sediments immediately overlying basement.
[d] Sediments intercalated within basement.

Table 4. Chemical composition of sediments, Site 482.

| | Sample (interval in cm) | | | | | | | | | | | | | |
| | 482A-3-1, 103-106 | | 482B-9-3, 123-125 | | | 482B-10-7, 4-6[a] | 482D-1-4, 120-123 | | | 482D-5-2, 60-63 | | 482D-7-3, 145-147[a] | | |
Component	Bulk	<2 μm	Bulk	2-20 μm	<2 μm	<2 μm	Bulk	2-20 μm	<2 μm	Bulk	<2 μm	Bulk	2-20 μm	<2 μm
SiO_2	53.96	51.40	55.12	59.80	54.92	59.78	52.66	61.60	53.60	57.02	54.74	57.80	65.31	52.86
TiO_2	0.58	0.79	0.58	0.60	0.64	0.64	0.62	0.62	0.77	0.62	0.73	0.66	0.56	0.85
Al_2O_3	14.35	17.70	14.88	13.98	13.46	15.48	15.39	13.66	16.67	15.56	18.09	17.18	13.85	20.28
Fe_2O_3	2.96	3.53	2.93	3.51	2.38	3.39	3.04	4.19	3.38	2.41	2.78	2.89	3.60	2.18
FeO	1.29	1.46	1.29	1.09	1.60	1.26	1.77	0.67	1.47	1.43	1.36	2.04	1.07	2.48
MnO	0.06	0.07	0.12	0.12	0.16	0.08	0.05	0.07	0.05	0.08	0.06	0.05	0.04	0.03
MgO	2.92	3.06	2.90	2.49	4.18	2.74	2.09	1.61	2.66	2.90	2.98	2.34	2.01	3.71
CaO	3.35	0.78	2.58	1.57	1.34	0.67	3.69	1.45	0.67	3.58	1.01	2.57	0.67	0.11
Na_2O	2.84	0.87	2.36	1.67	0.87	1.50	2.83	3.17	0.82	2.60	0.62	2.08	2.09	0.90
K_2O	2.50	2.02	2.50	2.75	1.85	3.56	3.01	3.05	2.31	2.50	2.25	3.11	3.35	3.65
P_2O_5	0.26	0.18	0.26	0.20	0.22	0.18	0.14	0.31	0.19	0.24	0.15	0.18	0.22	0.14
LOI	14.6	18.1	13.9	11.7	17.8	10.5	14.30	9.10	16.8	10.7	14.9	8.90	6.70	12.40
Total	99.67	99.96	99.42	99.48	99.42	99.78	99.59	99.80	99.39	99.64	99.67	99.80	99.47	99.59
K_2O/Na_2O	0.88	2.32	1.06	1.64	2.13	2.37	1.06	0.96	2.82	0.96	3.63	1.50	1.60	4.06
$K_2O + Na_2O/Al_2O_3$	0.37	0.16	0.33	0.32	0.20	0.33	0.38	0.46	0.19	0.33	0.16	0.30	0.39	0.22
$Fe_2O_3 + FeO + MgO/Al_2O_3$	0.50	0.45	0.48	0.51	0.61	0.48	0.45	0.47	0.45	0.43	0.39	0.42	0.48	0.41
SiO_2/Al_2O_3	3.76	2.90	3.70	4.28	4.08	3.86	3.42	4.51	3.21	3.66	3.02	3.36	4.71	2.61
Fe	3.08	3.61	3.06	3.31	2.91	3.35	3.51	3.45	3.51	2.80	3.01	3.61	3.35	3.46
Al/Ti	21.71	19.96	22.54	20.58	18.76	21.58	22.02	19.57	19.19	22.30	21.79	23.33	21.59	21.08

Note: Values shown in weight percent.
[a] Sediments immediately overlying basement.
[b] Sediments intercalated within basalts.

sediments within basalts. Cu, Cr, and V are somewhat concentrated in the clay fraction as compared with bulk samples but Ni and Pb are lower in the clay fraction.

Most of the trace elements, except for Cr and V, are relatively enriched in the intermediate fraction (Table 5), and the composition of this fraction is quite variable, depending clearly on the location of samples in the sediment section relative to basalts. A sharp increase in Cu, Zn, and Ag concentrations in the fraction coincides with the presence of authigenic pyrite, so we assume that most of the trace elements are associated with this mineral. An alternative or additional association may exist between the trace elements and Fe–montmorillonite, relatively more abundant in the intermediate fraction.

There is a rather irregular though apparent downhole increase in Cu, Ni, V, Pb, Zn, and Ag content and a less obvious increase in Co and Sn content; there is no increase in B, Cr, and Mo. Except for Mo, the highest concentrations of the trace elements were detected in the 2-20 μm fraction of Sample 482B-10-5, 102–104, about 2 meters above the basement, where Cu content is as high as 850 ppm; Ni, 900 ppm; Ag, 6.0 ppm; Sn, 63 ppm; and Pb, 129 ppm. In smear slide, this sample is observed to be a common silty clay, which contains about 2% pyrite. The clay fraction from sediment/basalt contacts and layers intercalated within basalts are less enriched in the trace elements, although average trace element values for these sediments (Table 5) are higher, than those for the upper portion of the section. Hydrothermal redistribution may explain the enrichment in trace elements of lower parts of the section along with reducing conditions, resulting in pyrite precipitation.

SITE 483

Site 483 is located 52 km west of the crest of the East Pacific Rise and about 25 km east of Baja California continental slope. Thickness of sediments above basaltic basement is 110 meters. These are Quaternary, hemipelagic silty clays, lithologically similar to those at Site 482. The layers intercalated within basalts are of late Pliocene age. In Hole 483C temperature measured at the base of the sediments was 30°C.

We studied sediment samples from Holes 483 and 483B. Two of these are from layers intercalated within basalt (Samples 483-18-2, 55–57 cm and 483-19-4, 63–65 cm); another two were taken from just above the basement (Samples 483-13-3, 50–52 cm, 1 meter above the contact and 483B-2-6, 93–97 cm, 0.5 m above the contact with uppermost basalts).

Mineralogy

The mineralogy of the Site 483 sediments, as determined in smear slides and thin sections is similar to that at Site 482. The sediments are composed mainly of terrigenous clay minerals, quartz, feldspars, and mica flakes with minor admixtures of biogenic calcite and opal in the upper part of the section, and minor organic matter fragments and authigenic pyrite throughout.

Pyrite occurs throughout the sediment section, but in our samples from Unit I we found less than 1% by volume of the mineral (according to visual estimation in smear slides), whereas in Unit III below 70 meters subbottom it is much more abundant (up to 4–6%). In some samples the pyrite aggregates display the shape of barite crystals. These may be either skeletal crystals of barite or pyrite pseudomorphs after barite.

Barite was found in thin sections and smear slides of samples taken just above basement (Samples 483-12-3, 88–90 cm, 483-13-3, 50–52 cm, and 483B-2-6, 93–97 cm) and from sediments intercalated within basalt (Sample 483-18-2, 55–57 cm). In thin section the mineral occurs as radial spherulitic aggregates, 0.3 to 0.7 mm in diameter. The platy crystals of barite contain numerous clay particles and pyrite. In a smear slide (Sample 483-12-3, 88–90 cm), we observed a euhedral barite crystal, 0.05

Table 4. (Continued).

			Sample (interval in cm)						Sediments Overlying Basement Av. Comp.		
482D-9-1, 3-7[b]			482F-3-4, 88-90			482F-4-3, 46-49	482F-4-3, 100-102[a]		Bulk	2-20 μm	<2 μm
Bulk	2-20 μm	<2 μm	Bulk	2-20 μm	<2 μm	<2 μm	Bulk	2-20 μm	(n = 5)	(n = 3)	(n = 6)
56.18	65.10	54.55	53.34	62.90	54.25	53.87	54.28	62.31	54.42	61.43	53.80
0.64	0.56	0.81	0.64	0.58	0.68	0.73	0.60	0.60	0.61	0.60	0.72
16.43	14.28	19.99	14.95	15.42	18.89	18.13	16.46	14.88	15.03	14.35	17.16
3.06	3.66	1.89	3.90	4.05	3.02	2.88	3.46	4.32	3.05	3.92	3.00
1.87	1.47	2.68	1.43	0.87	1.47	1.27	1.33	0.94	1.44	0.88	1.44
0.07	0.05	0.04	0.06	0.04	0.03	0.04	0.06	0.04	0.07	0.08	0.07
2.01	1.85	3.06	2.28	1.29	2.50	2.42	2.21	1.85	2.62	1.80	2.97
4.37	0.56	0.45	3.92	0.89	0.45	1.23	3.69	0.34	3.42	1.30	0.91
2.25	2.09	0.98	2.27	2.25	0.86	0.78	2.27	1.92	2.58	2.36	0.80
3.02	3.35	3.55	3.32	3.55	3.05	3.45	3.22	4.25	2.77	3.12	2.49
0.12	0.15	0.18	0.19	0.24	0.27	0.15	0.18	0.27	0.22	0.25	0.39
9.50	6.70	11.40	13.20	7.50	13.90	14.50	11.9	7.9	13.34	9.43	16.00
99.52	99.82	99.58	99.50	99.58	99.32	99.45	99.66	99.62			
1.34	1.60	3.62	1.46	1.58	3.55	4.42	1.42	2.21	1.08	1.39	3.14
0.32	0.38	0.23	0.37	0.38	0.21	0.23	0.33	0.41	0.36	0.39	0.15
0.42	0.49	0.38	0.51	0.40	0.37	0.36	0.42	0.48	0.47	0.46	0.44
3.42	4.56	2.73	3.56	4.08	2.87	2.97	3.29	4.18			
3.60	4.01	3.41	3.84	3.51	3.26	3.01	3.46	3.75			
22.92	22.94	22.06	20.84	23.34	24.41	21.84	24.22	21.88			

mm long, with a large pyrite spherule included. Carbonate crystals seem to replace barite in some cases.

Zeolite (clinoptilolite) occurs as small crystals and irregular grains in most smear slides, but its frequency is variable, and it disappears in the Pliocene sediments intercalated within the basement.

Carbonates of the dolomite–ankerite(?) group occur below 34 meters sub-bottom as very small rhombic crystals. Their frequency increases below 70 meters sub-bottom, but we have not found any samples with high concentrations of the minerals.

X-ray diffraction data for the clay and intermediate fractions show that clay mineral assemblage is similar to that of Site 482, but smectite content is lower and mica content is higher in the clay fraction and particularly in the intermediate fraction (Table 6). In a sample of near-surface sediments (4 m sub-bottom), mica even predominates over smectite. The sediments near basement and those intercalated within basalts show a slight increase in smectite in the clay fraction.

Clinoptilolite occurs in both fractions down to sediment/basement contact, but was not detected by x-ray diffraction in sediments intercalated within basalt. In several samples below 90 meters sub-bottom it is abundant.

Four samples of the coarse (>20 μm) fraction, from an interval 70 to 109 meters sub-bottom, were analyzed by the immersion method (Table 3) and found to contain 1.7 to 6.5% heavy minerals, somewhat more than we estimated at Site 482. Pyrite predominates in the heavy fraction (61-95%) in all samples. Other authigenic heavy minerals are virtually absent: we found only a single grain of barite. Terrigenous minerals are represented by the epidote group (which predominates), plus hornblende, zircon, and apatite with rare garnet, clinopyroxene, rutile, and sphene. The assemblage is similar to that at Site 482, but the hornblende content is somewhat higher.

The light fraction consists almost entirely of quartz and feldspars, the latter commonly predominating. Zeolite and gypsum were not found.

Geochemistry

In bulk samples, concentrations of the trace elements studied (Table 7) are similar (Cr, Mo, Sn) or higher (B, Co, Cu, Ni, V, Pb, Zn, Ag) than those at Site 482. Such elements as B, Cu, Mo, Ni, and Zn are more concentrated in the upper portion of the section, whereas sediments immediately overlying basement and within the basalt show lower concentrations. Other elements are either evenly distributed throughout the set of samples or show irregular variations irrespective of distance from basalts. The general order of relative abundance of elements at Site 483 is the same as at Site 482.

The intermediate fraction (2–20 μm) is relatively enriched in most of the trace elements studied, as compared with the clay fraction and with bulk samples, but the difference between the intermediate fraction and bulk sample composition is smaller than that at Site 482. We have not detected any clear trend toward increasing concentration in the fraction just above basement or intercalated within basalt. In fact, the average values of most trace elements are approximately equal to or even lower (B, Zn, Ag) than those for sediments recovered far above the basement or from corresponding levels within or immediately overlying the basement at Site 482. Vanadium alone regularly increases with depth in the clay fraction relative to the intermediate fraction.

The highest concentrations in the 2–20 μm fraction of zinc along with copper, nickel, and vanadium were detected in three samples from Cores 483-9 through 12 (70–100 m sub-bottom). Smear slides show that all these samples contain abundant pyrite. The maximum amounts of Zn (748 ppm), Cu (300 ppm), Ni (145 ppm), and V (160 ppm), as well as B (110 ppm), Co (18 ppm), Cr (71 ppm), and Pb (74 ppm) were determined in a sample of

Table 5. Trace element composition of sediments, Site 482.

Sample (interval in cm)	Sub-bottom Depth (m)	B	Co	Cr	Cu	Mo	Ni	V	Pb	Sn	Zn	Ag	Sc	Zr
Bulk samples														
Hole 482A														
3-1, 103–106	16.63	95	7	55	41	25	44	75	38	3	115	0.32		
Hole 482B														
2-2, 88–90	55.88	71	9	56	50	33	59	76	36	4	138	0.35		
7-2, 94–96	103.44	65	6	30	37	22	32	56	25	2	120	0.19		
9-6, 118–120	128.68	58	8	38	51	16	50	73	33	4	148	0.25		
10-4, 42–46	134.42	76	10	48	66	37	63	80	46	5	270	0.29		
10-5, 102–104	136.52	67	8	46	58	19	59	85	38	4	152	0.21		
10-7, 4–6[a]	138.54	56	10	48	55	18	50	81	42	4	178	0.23		
19-1, 47–49[b]	193.47	51	7	40	46	7	40	67	36	3	142	0.25		
Hole 482C														
7-6, 25–27	128.25	62	10	50	55	19	62	81	44	4	190	0.32		
9-1, 12–14[a]	132.12	40	8	35	43	13	48	68	32	3	160	0.25		
Hole 482D														
1-4, 120–123	77.20	112	7	48	43	18	50	77	28	3	135	0.29		
5-2, 60–63	111.60	72	9	55	45	22	50	87	46	4	126	0.32		
7-3, 145–147[a]	132.95	56	11	53	37	25	63	93	50	5	174	0.29		
9-1, 5–7[b]	141.53	51	9	44	46	18	49	82	38	4	195	0.27		
Hole 482F														
3-4, 88–90	128.38	65	10	40	44	16	44	77	33	3	148	0.25		
4-2, 38–40	133.88	65	8	43	48	18	50	84	36	3	195	0.23		
4-3, 46–49	135.46	62	8	40	46	15	48	81	33	3	142	0.23		
4-3, 100–102[a]	136.00	32	8	41	45	15	55	80	28	3	138	0.19		
Average:														
Sediments above basement (n = 12)		72	8	46	49	22	51	78	36	4	157	0.27		
Sediments just above basement (n = 4)		46	9	44	45	18	54	80	38	4	162	0.24		
Sediments intercalated within basalts (n = 2)		51	8	42	46	12	44	74	37	4	168	0.26		
2–20 μm sediment fraction														
Hole 482A														
3-1, 103–106	16.63	62	8	54	170	40	45	91	59	12	125	2.9		
Hole 482B														
2-2, 89–90	55.88	63	8	62	138	48	61	88	50	5	230	1.8		
7-2, 94–96	103.44	65	9	48	240	60	48	75	63	8	300	3.3		
9-6, 118–120	128.68	63	11	55	186	29	75	96	60	11	325	2.0		
10-4, 42–44	134.42	58	9	40	186	30	66	80	63	8	343	2.9		
10-5, 102–104	136.52	95	21	92	850	5	163	166	129	63	900	6.0		
10-7, 4–6[a]	138.54	70	16	61	380	39	110	113	83	14	576	5.1		
19-1, 47–49[b]	193.47	93	21	91	350	21	97	148	95	29	638	4.6		
Hole 482C														
7-6, 25–27	128.25	62	11	42	260	24	69	85	72	14	338	4.4		
9-1, 12–14[a]	132.12	65	12	53	290	26	86	94	68	10	315	4.7		
Hole 482D														
1-4, 120–123	77.20	114	11	67	229	40	69	115	63	8	282	4.0		
5-2, 60–63	111.60	63	11	54	186	33	58	86	59	9	308	2.3		
7-3, 145–147[a]	132.95	59	13	47	154	28	85	97	72	8	274	2.8		
9-1, 5–7[b]	141.53	69	14	50	286	29	90	101	80	14	404	6.6		
Hole 482F														
3-4, 88–90	128.38	61	12	43	190	35	61	89	69	7	245	2.0		
4-3, 46–49	135.46	51	11	54	138	28	73	87	55	6	270	2.2		
4-3, 100–102[a]	136.00	57	13	48	197	28	77	90	71	6	384	5.3		
Average:														
Sediments above basement (n = 11)		66	10	52	192	38	62	89	61	9	277	2.8		
Sediments immediately overlying basement (n = 4)		63	14	52	255	30	90	99	74	10	387	4.5		
Sediments intercalated within basalts (n = 2)		81	17	70	318	25	93	125	88	21	521	5.5		
Clay sediment fraction														
Hole 482A														
3-1, 103–106	16.63		—	27	120		23	110	20	—			14	200

Table 5. (Continued).

Sample (interval in cm)	Sub-bottom Depth (m)	B	Co	Cr	Cu	Mo	Ni	V	Pb	Sn	Zn	Ag	Sc	Zr
Clay sediment fraction (Cont.)														
Hole 482B														
2-2, 88–90	55.88	—		95	87		16	90	14	—			15	118
7-2, 94–96	103.44	8		45	190		18	86	16	2			23	110
9-6, 118–120	128.68	11		65	100		22	100	9	2			28	118
10-4, 42–44	134.42	—		120	68		24	100	17	—			13	165
10-5, 102–104	136.52	—		27	84		14	63	13	—			8	148
10-7, 4–6	138.54	5		36	100		16	71	15	2			12	93
19-1, 47–49	193.47	—		68	95		20	85	15	—			16	135
Hole 482C														
7-6, 25–27	128.25	—		200	120		45	240	15	—			30	180
9-1, 12–14	132.12	—		140	200		22	156	16	3			14	170
Hole 482D														
1-4, 120–123	77.20	—		166	150		50	116	17	4			22	120
5-2, 60–63	111.60	—		112	62		42	93	10	4			12	115
7-3, 145–147	132.95	—		93	64		22	140	9	—			19	140
9-1, 3–7	141.53	—		220	107		56	165	24	—			18	65
Hole 482F														
3-4, 88–90	128.38	—		87	65		50	70	38	—			15	190
4-2, 38–40	133.88	12		170	118		40	160	4	—			20	250
4-3, 41–49	135.46	—		130	130		60	125	12	7			27	135
4-3, 100–102	136.00	—		130	106		50	100	12	4			19	138
Average:														
Sediments above basement (n = 12)				104	108		34	113	15	4			19	154
Sediments immediately overlying basement (n = 4)				100	118		28	117	13	3			16	135
Sediments intercalated within basalts (n = 2)				144	101		38	125	20				17	100

Note: Values shown in ppm.
[a] Sediments just above basement.
[b] Sediments intercalated within basalts.
— = Not detected.

silty clay with about 6% pyrite (Sample 483-12-3, 88–90 cm). In this sample we found also barite and ankerite; small sphaelerite(?) crystals may be present.

SITE 484

The holes at Site 484 were drilled on a basement "diapir" that was covered by 50 meters of thick upper Quaternary hemipelagic mud. The sedimentation rate is about 110 m/m.y. We studied four samples from Hole 484A. The lowermost sample, 484A-6-5, 23–25 cm, was taken within 3 meters of the basement.

Mineralogy

The mineralogy of the sediments, as determined in smear slides, differs from that at Sites 482 and 483 by higher biogenic opal content and by less abundant terrigenous quartz and feldspars. The upper three samples studied (Section 3 in Cores 1, 3, and 6) are siliceous clay, siliceous silty clay, and nannofossil ooze, respectively, whereas Sample 484A-6-5, 23–25 cm, taken just above basement, contains only a minor admixture of poorly preserved (dissolved?) radiolarians. In this sample we observed irregular aggregates of an opal-like mineral, possibly authigenic opal, formed after biogenic silica dissolution. Pyrite content is low (commonly less than 1%). In all samples we found authigenic carbonates (dolomite-ankerite?), zeolite, and rare barite. Biogenic phosphate occurs sporadically.

X-ray diffraction data (Table 8) show that the mineralogy of the clay fraction is similar to that in Holes 482A and 482B. Smectite strongly predominates over mica with minor admixtures of chlorite and kaolinite. In coarser fractions, smectite content is much lower—equal to or even less than that of mica. Only in the lowermost sample does smectite predominate. Clinoptilolite was detected in the clay and intermediate fractions of all samples. In the three upper samples of the 2–20 μm fraction, it is abundant.

A single coarse fraction analysis of Sample 484-6-5, 23–25 cm (just above basement) shows 2.4% heavy minerals, 93% of which consists of pyrite. The rest are hornblende, epidote, zircon, and apatite. The light fraction is composed of almost equal amounts of quartz and feldspars with abundant aggregates and pellets of clay. Zeolite was not found in this fraction.

Geochemistry

Bulk analyses of two samples (Table 9) show that sediments near the basalts and far above are chemically quite similar, resembling those in the upper part of the section at Site 482. The 2–20 μm fraction is more enriched in SiO_2, CaO, and Na_2O, whereas Al_2O_3, FeO, MgO, and the K_2O to Na_2O ratio tend to increase in the clay fraction. The SiO_2 to Al_2O_3 ratio is somewhat higher in the coarse fraction as a result of its more abundant biogenic silica, and the Al to Ti ratio is close to that of average terrigenous matter.

409

Table 6. Mineralogy of the 2-20 μm and clay sediment fractions, Site 483 (in percent).

Sample (interval in cm)	Sub-bottom Depth (m)	Lithology	Age	Smectite	Mica	Chlorite	Mixed-layer Chlorite-Montmorillonite	Z	Quartz	Clinoptilolite	Amorphous Phase	Feldspar
Intermediate (2–20 μm) sediment fraction												
Hole 483												
2-3, 10–12	4.10	Unit II	Upper Quaternary	20	70	10		0.6	d	c	c	d
5-3, 131–133	33.81	Diatomaceous mud and ooze, muddy nannofossil ooze		45	45	10		0.7	d	c	c	d
7-5, 90–92	55.40			58	36	6	tr	0.6	d	c	c	c
9-2, 60–62	69.60	Unit III	Lower Quaternary	75	20	5	tr	0.6	c	c	tr	c
10-2, 5–8	78.55	Clay and silty clay		57	36	7	tr	0.6	c	c	tr	c
11-4, 110–113	92.10			60	22	8		0.6	c	d	tr	c
12-3, 88–90	99.80			70	24	6	tr	0.6	c	c	tr	c
13-1, 120–122	106.70			58	34	8	tr	0.7	d	d	c	d
13-2, 110–112	108.10			69	25	6	tr	0.7	c	c	tr	c
13-3, 50–52	109.00			59	35	6	tr	0.7	d	c	c	d
18-2, 55–57[b]	153.05	Silty clay, siltstone, and claystone	Upper Pliocene	56	29	15	tr	0.7	d		tr	c
18-4, 63–65[b]	156.13			68	18	14	tr	0.6	d		tr	d
Hole 483B												
2-6, 93–97[a]	109.43	Unit I Silty clay	Quaternary	54	38	8		0.7	d	d	tr	d
Clay sediment fraction												
Hole 483												
2-3, 10–12	4.10	Unit I	Upper Quaternary	68	24	8	tr	0.4	tr	c	tr	tr
5-3, 131–133	33.81	Diatomaceous mud and ooze,		71	23	6		0.4	tr	c	tr	tr
7-5, 90–92	55.40	muddy nannofossil ooze		75	13	12		0.6	tr	c	tr	tr
9-2, 60–62	69.60	Unit III		79	16	5	tr	0.5	tr	c	tr	tr
10-2, 5–8	78.55	Clay and silty clay	Lower Quaternary	70	21	9		0.5	tr	c	tr	tr
11-4, 110–113	92.10			78	18	4	tr	0.5	tr	c	tr	tr
12-3, 88–90	99.80			57	38	5	tr	0.3	tr	c	tr	tr
13-1, 120–122	106.70			75	19	6		0.5	tr	c	tr	tr
13-2, 110–112	108.10			75	23	2		0.5	tr	c	tr	tr
13-3, 50–52	109.00			84	14	2		0.6	tr		tr	tr
18-2, 55–57[b]	153.05			73	19	8		0.5	tr		tr	tr
18-4, 63–65[b]	156.13	Silty clay, siltstone, and claystone	Upper Pliocene	78	15	7		0.5	tr		tr	tr
Hole 483B												
2-6, 93–97[a]	109.43	Unit I Silty clay	Quaternary	78	15	7		0.4	tr	c	tr	tr

[a] Sediment immediately overlying basement.
[b] Sediments intercalated within basalts.
[c] Moderate.
[d] Abundant.

Trace elements in the three upper samples (Table 10) occur approximately in the same concentrations as in sediments far above the basement at Site 482. But in Sample 484A-6-5, 23–25 cm (just above basement) concentrations of most elements (except for Cr, Mo, and Sn), both in bulk samples and particularly in the 2–20 μm fraction, are markedly higher. Zn, Ag, Cu, V, Ni, B, and Co concentrations in this sample are close to those in most enriched samples from Site 483 and to those from sediments in the basement at Site 482.

SITE 485

Site 485 is located about 10 km southeast of Site 482 on Quaternary crust overlain by 150 meters of lower and upper Quaternary hemipelagic clay mixed with clayey silt and silty sand in the lower part of the section. The site, located near the continental slope of mainland Mexico, is characterized by an extremely high sedimentation rate, about 625 m/m.y. Several layers of lower Quaternary sediments were recovered intercalated within basalts in the depth interval from 160 to 330 meters sub-bottom, including lithified clayey siltstones, sandstones, and claystones. High heat-flow values were measured at the site.

We studied sediments from Holes 485 and 485A. In the latter, 18 samples are from layers intercalated within basalts, and one sample (485A-11-3, 35–37 cm) was taken 20 cm above the sediment/basalt contact.

Mineralogy

The mineralogy of Site 485 sediments, as determined by smear-slide and thin-section analysis, is similar to that at the other sites drilled on Leg 65. Terrigenous clay minerals and silt-size quartz and feldspars predominate throughout the section, including the sediment layers within basement. Minor biogenic minerals—opal (diatoms, radiolarians, sponge spicules) and calcite (foraminifers, nannofossils)—are unevenly distributed throughout the section. Diatoms and radiolarians are relatively abundant in the upper Quaternary sediments (Hole 485, Cores 1 through 6). Below 50 meters sub-bottom they become rare, and they virtually disappear below 80 meters. Biogenic calcite occurs throughout, but high concentrations were found only in several samples from layers intercalated within basement (Hole 485A, Cores 20, 22, 36). We detected these authigenic minerals in sediments: pyrite, zeolite (clinoptilolite), carbonates (dolomite-ankerite), barite, gypsum, and opal(?).

Pyrite occurs throughout the section. In the upper portion of the section above the basalts, pyrite content is commonly low, about 1% or less, according to visual estimation in smear slides. It is represented mainly by

Table 7. Trace element composition of sediments, Site 483.

Sample (interval in cm)	Sub-bottom Depth (m)	B	Co	Cr	Cu	Mo	Ni	V	Pb	Sn	Zn	Ag	Sc	Zr
Coarse sediment														
Hole 483														
2-3, 10–12	4.10	102	17	62	119	19	118	104	55	3	250	0.32		
5-3, 131–133	33.81	107	15	50	112	82	85	83	50	3	210	0.37		
9-2, 60–62	69.60	115	19	63	144	24	167	118	56	4	440	0.45		
11-4, 110–113	92.10	110	15	50	97	10	116	108	38	3	265	0.29		
12-3, 88–90	99.80	110	18	56	125	9	161	126	46	3	310	0.48		
13-1, 120–122	106.70	100	14	62	76	25	114	108	50	4	215	0.29		
13-3, 50–52[a]	109.00	72	11	46	87	10	119	96	40	3	230	0.45		
18-2, 55–57[b]	153.05	87	9	50	55	11	50	90	42	4	142	0.27		
18-4, 63–65[b]	156.13	107	11	56	68	12	90	85	40	4	158	0.35		
Hole 483B														
2-6, 93–97[a]	109.43	95	12	44	84	19	82	101	40	3	174	0.29		
Average:														
Sediments above basement (n = 6)		107	16	57	112	28	127	108	49	3	282	0.37		
Sediments just above basement (n = 2)		83	11	45	85	14	100	98	40	3	202	0.37		
Sediments intercalated within basalts (n = 2)		97	10	53	62	11	70	87	41	4	150	0.31		
2–20 μm sediment fraction														
Hole 483														
2-3, 10–12	4.10	42	11	26	179	45	47	71	40	8	353	4.6		
5-3, 131–133	33.81	48	9	28	260	52	49	62	44	24	453	6.0		
9-2, 60–62	69.60	67	12	33	200	5	92	92	40	9	605	3.8		
11-4, 110–113	92.10	63	11	37	215	12	104	97	60	8	633	4.5		
12-3, 88–90	99.80	110	18	71	300	7	145	160	74	12	748	3.8		
13-1, 120–122	106.70	54	8	37	120	105	43	81	42	9	260	4.4		
13-3, 50–52[a]	109.00	50	9	37	170	12	79	80	52	13	470	4.1		
18-2, 55–57[b]	153.05	51	11	48	200	12	40	87	46	14	303	3.8		
18-4, 63–65[b]	156.13	63	11	53	230	28	73	92	72	6	328	4.0		
Hole 483B														
2-6, 93–97[a]	109.43	44	7	30	81	32	46	67	36	8	158	1.8		
Average:														
Sediments above basement (n = 6)		64	12	39	212	38	80	94	50	12	509	4.5		
Sediments just above basement (n = 2)		47	8	34	125	22	62	74	44	10	314	3.0		
Sediments intercalated within basalts (n = 2)		57	11	50	215	20	56	90	59	10	315	3.9		
Clay sediment fraction														
Hole 483														
2-3, 10–12	4.10			1	48		58	150	—				6	100
5-3, 131–133	33.81	160	47	36	54	34	54	110	9	5	110	8.4	8	120
9-2, 60–62	69.60			56	65		79	220	21				11	153
11-4, 110–113	92.10			48	69		72	150	14				10	178
13-1, 120–122	106.70			60	42		39	100	6				12	118
13-3, 50–52[a]	109.00	66	15	52	60	12	85	140	12	6	380	8.0	17	110
18-2, 55–57[b]	153.05			150	100		40	140	13				18	105
18-4, 63–65[b]	156.13	99	13	90	70	16	45	95	9	5	340	5.5	14	93
Hole 483B														
2-6, 93–97[a]	109.43			75	55		49	200	15				18	138
Average:														
Sediments above basement (n = 5)				50	56		60	146	12				9	134
Sediments just above basement (n = 2)				64	57		67	170	14				18	124
Sediments intercalated within basalts (n = 2)				120	85		42	117	11				16	99

Note: Values shown in ppm.
[a] Sediments just above basement.
[b] Sediments intercalated within basalts.
— = Not detected.

411

Table 8. Mineralogy of clay and intermediate sediment fractions, Site 484 (in percent).

Sample (interval in cm)	Sub-bottom Depth (m)	Lithology	Age	Smectite	Mica	Chlorite	Mixed-layer Chlorite–Montmorillonite	Z	Quartz	Clinoptilolite	Amorphous Phase	Feldspar
Clay (<2 μm) sediment fraction												
Hole 484A												
1-3, 130–134	4.30	Unit I Siliceous clay	Upper Quaternary	78	14	8		0.5	tr	b	tr	tr
3-3, 110–114	21.60	Unit II		65	27	8	tr	0.3	tr	b	tr	tr
6-3, 110–114	50.10	Siliceous silty clay, clayey		74	18	8	tr	0.4	tr	b	tr	tr
6-5, 23–25	52.23[a]	siliceous ooze and nannofossil ooze		65	26	9	tr	0.6	tr	b	tr	tr
Intermediate (2–20 μm) sediment fraction												
Hole 484A												
1-3, 130–134	4.30	Unit I Siliceous clay	Upper Quaternary	48	48	4	tr	0.7	c	c	b	c
3-3, 110–114	21.60	Unit II		42	52	6	tr	0.7	c	c	b	c
6-3, 110–114	50.10	Siliceous silt clay, clayey		45	45	10	tr	0.7	c	c	b	c
6-5, 23–25	52.23[a]	siliceous ooze and nannofossil ooze		66	29	5	tr	0.5	b	b	tr	b

[a] Sediments just above basement.
[b] Moderate.
[c] Abundant.
[d] Tr = trace.

Table 9. Chemical composition of sediments, Hole 484A.

	Sample (interval in cm)					
	484A-1-3, 130–134			484A-6-5, 23–25[a]		
Component	Bulk	2–20 μm	<2 μm	Bulk	2–20 μm	<2 μm
SiO_2	52.94	65.84	54.30	50.10	61.96	54.90
TiO_2	0.51	0.51	0.60	0.51	0.54	0.62
Al_2O_3	12.95	13.61	15.96	13.56	14.33	15.99
Fe_2O_3	3.31	2.97	3.80	3.87	3.40	3.24
FeO	1.46	0.87	1.67	1.02	0.80	1.34
MnO	0.11	0.07	0.07	0.10	0.07	0.06
MgO	2.18	1.53	2.34	2.18	2.01	2.90
CaO	5.15	1.79	0.89	5.60	1.45	0.34
Na_2O	3.20	2.25	0.98	2.83	2.09	0.94
K_2O	2.40	2.95	2.59	2.70	3.05	2.68
P_2O_5	0.18	0.19	0.15	0.13	0.27	0.22
LOI	15.10	7.10	16.60	17.30	9.90	16.10
Total	99.49	99.68	99.95	99.90	99.87	99.33
K_2O/Na_2O	0.75	1.31	2.64	0.95	1.46	2.85
$K_2O + Na_2O/Al_2O_3$	0.43	0.38	0.22	0.41	0.36	0.23
$Fe_2O_3 + FeO + MgO/Al_2O_3$	0.54	0.39	0.49	0.52	0.43	0.47
SiO_2/Al_2O_3	4.09	4.84	3.40	3.69	4.32	3.43
Fe	3.46	2.76	3.96	3.50	3.00	3.31
Al/Ti	22.13	23.26	23.5	23.19	23.72	22.89

Note: Values shown in weight percent.
[a] Sediment immediately overlying basement.

microspherules several micrometers in diameter. Relatively rich in pyrite (2%) are samples from Sections 485-4-2, and 485A-8-2. Abundant pyrite (3–5%) was found in some samples from the layers within basement: from Cores 19, 20, 28, 37, 38 of Hole 485A (for sample identification see Table 11). However, in many other samples from those layers intercalated within basalts, pyrite content is rather low: 1% or less. So the layers do not show any regular increase in pyrite associated with hydrothermal activity. Pyrite occurs as cubic crystals, crystal aggregates, dendritic forms, and as pseudomorphs after fragments of organic material and other sedimentary particles. Spherules are rather rare and some of those show evidence of recrystallization (rounded contours turn into multiangular ones).

Zeolite (clinoptilolite) occurs as platy crystals or irregular grains with clay inclusions in sediments above the uppermost basalt (down to 158 m sub-bottom). In sediments within basement we found rare colorless grains with a low refractive index, possibly analcime. The mineral is common in Sample 485A-39-1, 94–96 cm, where analcime was identified by x-ray diffraction.

Authigenic carbonates occur as small (1–5 μm or less) rhombohedral crystals and irregular grains. Grains with a high refractive index along both axes seem to be ankerite, whereas those with one index less than 1.54 are likely to be dolomite or calcite. The authigenic carbonates are more abundant in the sediment section above basalts. In some samples their concentration is visually up to 1–2% (Hole 485A, Cores 6, 9, 11). In the layers within basement we found carbonates mainly in trace amounts, most of those being dolomite or calcite.

However, in two samples from Section 485A-2-1, we observed in thin sections spheroidal poikiloblastic crystal aggregates of a carbonate mineral (dolomite?) 0.05 to 0.5 mm in diameter. The crystals are filled with sediment particles, such as clay minerals, quartz, and plant debris, which show a primary orientation subparallel to bedding. The same samples contain authigenic mixed-layer clay minerals and analcime.

Barite is rare in the sediments at this site. We observed rare crystals of the mineral in a sample from Section 485-3-4 and in several others. In two thin sections from Hole 485A, Core 20 we found a single barite spherulite in each. In most samples the mineral is absent.

Gypsum was identified with certainty in only one smear slide (Sample 485A-11-2, 107–111 cm), where we observed a "swallow-tail" twin, but most likely the mineral is present in several other samples as well.

Opal(?) occurs as irregular colorless isotropic grains with a low refractive index in several smear slides from the lower portion of the sediment section above and within basement. The shape suggests that the mineral was formed as an interstitial filling during initial lithification of wet sediments. Our identification of the mineral is, however, uncertain.

The mineralogy of the sediments recovered above the basement, as determined by x-ray diffraction, is similar to that of the hemipelagic sediments at Sites 482, 483,

Table 10. Trace element composition of sediments, Hole 484A.

Sample (interval in cm)	Sub-bottom Depth (m)	B	Co	Cr	Cu	Mo	Ni	V	Pb	Sn	Zn	Ag	Sc	Zr
Bulk sediments														
Hole 484A														
1-3, 130–134	4.30	83	11	43	71	16	71	72	33	3	134	0.48		
3-3, 110–114	21.60	87	9	44	71	14	65	78	31	2	148	0.46		
6-3, 110–114	50.10	100	12	44	77	10	79	78	42	3	220	0.40		
6-5, 23–25[a]	52.23	120	14	55	112	10	77	92	59	4	240	0.55		
Average: Sediments above basement ($n = 3$)		90	11	44	73	13	72	76	35	3	167	0.45		
2–20 μm sediment fraction														
Hole 484A														
1-3, 130–134	4.30	70	11	42	193	10	51	90	48	9	468	4.2		
3-3, 110–114	21.60	50	7	29	170	17	40	61	36	3	275	3.5		
6-3, 110–114	50.10	56	9	32	260	6	48	70	36	11	400	4.0		
6-5, 23–25[a]	52.23	125	23	44	358	5	104	139	74	8	636	6.5		
Average: Sediments above basement ($n = 3$)		59	9	34	208	11	46	74	40	8	381	3.9		
Clay sediment fraction														
Hole 484A														
1-3, 130–134	4.30		15	46	74		45	110	11	—			17	130
3-3, 110–114	21.60	260	16	89	68	4	36	125	14	4		2.1	16	125
6-3, 110–114	50.10		—	100	125		48	120	6	—			20	100
6-5, 23–25[a]	52.23	77	13	72	130	3	40	70	12		330	1.6	15	79
Average: Sediments above basement ($n = 3$)			15	78	89	4	43	118	16	4		2.1	26	127

Note: Values shown in ppm.
[a] Sediments just above basement.

and 484, but specific differences appear in some sediments intercalated within basalts.

In the clay fraction (Table 11), the clay mineral assemblage above basement is composed predominantly of smectite, which increases somewhat downhole up to 92% at 158 meters sub-bottom (near the basement). Mica and chlorite + kaolinite constitute the rest, showing irregular variations with depth. Quartz and feldspars occur as a minor admixture throughout. Clinoptilolite was detected in all samples above the basement. The clay mineral assemblage in the sediments within basement down to 231 m sub-bottom, as well as in the interval from 296 to 305 meters, is identical to that in the overlying sediments, but smectite content is commonly higher (80–94%) and chlorite + kaolinite is extremely low (2–8%). In three samples (236 m and 314 m sub-bottom), however, the clay minerals are quite different: pure smectite is absent, mica increases to 25%, and mixed-layer mica–montmorillonite and chlorite–montmorillonite predominate. Clinoptilolite was not found, but in the two lowermost samples we detected analcime.

The 2–20 μm fraction (Table 11) contains the same clay minerals as the clay fraction but smectite content is lower and mica content is markedly higher, particularly above 128 meters sub-bottom. Quartz, feldspars, and clinoptilolite are also more abundant. Mixed-layer minerals and analcime occur in the same samples in which they occur in the clay fraction. The coarse fraction (Table 11) is similar in composition to the 2–20 μm fraction, but quartz, feldspars, clinoptilolite, and amorphous phases are even more abundant. As in the case of the clay fraction, clinoptilolite disappears in the sediments intercalated within the basement in both the 2–20 μm and coarse fractions.

Mica in all samples is represented mainly by polytype 1M, whereas 2M occurs as a minor admixture (Table 12). Smectites in the upper portion of the section are predominantly Al–Fe–montmorillonites, but Fe–montmorillonite is also identified by b repeat distances of 9.04–9.05 Å (Table 12) and by treatment with hot 10% HCl (Table 2). Below 79 meters sub-bottom, the basal reflection peak of the smectites broadens markedly on diffraction diagrams. In sediments just above and within basement, Fe–montmorillonite is more abundant, particularly in the 2–20 μm fraction. The smectites commonly show "cloudy" appearance, but elongated platy (ribbon-like) crystals also occur. Just above the basement the authigenic clay minerals display a fused or sintered(?) texture (Plate 2, Fig. 5).

Along with predominating smectites in these sediments intercalated within basalts, at sub-bottom depths of 236 and 313 meters, we identified mixed-layer minerals: mica–montmorillonite and chlorite–montmorillonite, together with analcime (Tables 11). The mixed-layer mica–montmorillonite (Sample 485A-28-1, 148–150 cm) has in the dry state a peak at 11.3 Å, which moves after treatment with glycol to 14.7 Å, and after heating at 550°C to 10 Å. This mineral is insoluble in 10% HCl (Table 2). Heated samples show an additional peak at 10.6 Å, which corresponds to a mixed-layer chlorite–montmorillonite. On transmission electron photomicrographs, the mixed-layer minerals occur as flat elongated crystals (Plate 1, Fig. 4). SEM photomicrographs show

Table 11. Mineralogy of sediment fractions, Site 485 (in percent).

Sample (interval in cm)	Sub-bottom Depth (m)	Lithology	Age	Smectite	Mica	Chlorite	Mixed-layer Mica–Montmorillonite	Mixed-layer Chlorite–Montmorillonite	Z	Quartz	Clinoptilolite	Amorphous Phase	Feldspar	Analcime
Clay (< 2 μm) sediment fraction														
Hole 485														
1-2, 90–94	2.40	Unit IA	Upper Quaternary	65	26	9		tr	0.5	tr	c	tr	tr	
3-4, 120–124	18.20	Silty clay		76	17	7			0.4	tr	c	tr	tr	
4-2, 120–124	24.70			80	7	13		tr	0.4	tr	c	tr	tr	
6-4, 110–114	46.60	Unit IB Silty clay and nannofossil-bearing silty clay	Lower(?) Quaternary	75	16	9		tr	0.5	tr	c	tr	tr	
Hole 485A														
1-5, 120–124	52.10			73	14	13		tr	0.4	tr	c	tr	tr	
4-1, 63–66	79.63			75	15	10		tr	0.5	tr	c	tr	tr	
5-3, 111–115	92.61	Unit II		77	15	8		tr	0.6	tr	c	tr	tr	
6-3, 11–15	101.11	Silty clay and turbidites		76	14	10			0.5	tr	c	tr	tr	
8-2, 114–118	119.64			73	18	9		tr	0.5	tr	c	tr	tr	
9-1, 128–132	127.78			78	15	7			0.5	tr	c	tr	tr	
10-2, 104–107	138.54			88	9	3		tr	0.6	tr	c	tr	tr	
11-2, 107–111	148.07			84	13	3			0.6	tr	c	tr	tr	
11-3, 35–37[a]	158.35			92	6	2			0.5	tr	c	tr	tr	
19-2, 40–42[b]	189.90			66	25	9			0.6	tr	c	tr	tr	
20-1, 33–35[b]	192.83	Sandy mud, muddy		81	13	6			0.6	tr		tr	tr	
20,CC[b]	197.02	nannofossil chalk, and		80	12	8			0.7	tr		tr	tr	
22-2, 24–26[b]	203.24	nannofossil-bearing		89	8	3			0.7	tr		tr	tr	
22-4, 33–36[b]	206.33	silty claystone		90	7	3			0.6	tr		tr	tr	
22-6, 45–48[b]	209.45			92	6	2			0.6	tr		tr	tr	
26-1, 48–50[b]	226.48			90	7	3			0.7	tr		tr	tr	
27-1, 46–48[b]	230.96			87	9	4			0.6	tr		tr	tr	
28-1, 148–150[b]	236.48				25	10	45	20		tr		tr	tr	
34-1, 33–35[b]	277.33			47	35	18			0.2	tr		tr	tr	
36-1, 61–65[b]	295.61			91	6	3			0.6	tr		tr	tr	
36-2, 58–61[b]	297.08			88	8	4			0.6	tr		tr	tr	
36-3, 41–49[b]	298.41			94	4	2			0.6	tr		tr	tr	
37-1, 62–65[b]	304.62			94	4	2			0.5	tr		tr	tr	
38-1, 94–96[b]	313.94				25	15		60			c	tr	tr	c
38-1, 98–100[b]	313.98			tr	25	15		60			c	tr	tr	c
Intermediate (2–20 μm) sediment fraction														
Hole 485														
1-2, 90–94	2.40	Unit IA	Upper Quaternary	54	36	10		tr	0.7	d	d	tr	c	
3-4, 120–124	18.20	Silty clay		55	35	10		tr	0.6	d	d	tr	c	
4-2, 120–124	24.70			57	34	9		tr	0.5	d	c	tr	c	
6-4, 110–114	46.60	Unit IB Silty clay and nannofossil-bearing silty clay	Lower(?) Quaternary	50	37	13		tr	0.6	d	c	tr	c	
Hole 485A														
1-5, 120–124	52.10			65	22	13		tr	0.7	d	c	tr	c	
3-2, 5–9	71.05			73	17	10		tr	0.6	d	c	tr	c	
4-1, 63–66	79.63			67	23	10		tr	0.5	c	c	tr	c	
5-3, 111–115	92.61	Unit II		45	36	19		tr	0.6	d	c	tr	d	
6-3, 11–15	101.11	Silty clay and turbidites		48	38	14		tr	0.7	d	c	tr	c	
8-2, 114–118	119.64			58	28	14		tr	0.6	d	c	tr	c	
9-1, 128–132	127.78			64	24	12		tr	0.7	d	c	tr	c	
10-2, 104–107	138.54			72	20	8		tr	0.6	d	c	tr	c	
11-2, 107–111	148.07			81	15	4		tr	0.7	c	c	tr	c	
11-3, 35–37[a]	158.35			75	20	5		tr	0.7	c	c	tr	c	
19-2, 40–42[b]	189.90	Sandy mud, muddy		79	14	7		tr	0.6	c	tr	tr	c	
20-1, 33–35[b]	192.83	nannofossil chalk, and		78	15	7		tr	0.7	c		tr	c	
20,CC[b]	197.02	nannofossil-bearing		74	17	9		tr	0.7	d		tr	c	
22-2, 24–26[b]	203.24	silty claystone		78	18	4		tr	0.6	c		tr	c	
22-4, 33–36[b]	206.33			75	17	8		tr	0.6	c		tr	c	
22-6, 45–48[b]	209.45			70	19	11		tr	0.6	d		tr	c	
26-1, 48–50[b]	226.48			83	11	6		tr	0.6	c		tr	c	
27-1, 46–48[b]	230.96			80	12	8		tr	0.6	c		tr	c	
28-1, 148–150[b]	236.48				20	10	50	20		d		tr	c	
34-1, 33–35[b]	277.33			44	40	16		tr	0.5	d		tr	c	
36-1, 61–65[b]	295.61			82	13	5		tr	0.4	c		tr	c	
36-2, 58–61[b]	297.08			77	18	5		tr	0.7	c		tr	c	
36-3, 41–49[b]	298.41			78	16	6		tr	0.6	d		tr	c	
37-1, 62–65[b]	304.62			81	12	7		tr	0.5	c		tr	c	
38-1, 94–96[b]	313.94				25	15		60		d		tr	c	
38-1, 98–100[b]	313.98				28	17		55		d		tr		
Coarse (> 20 μm) sediment fraction														
Hole 485														
1-2, 90–94	2.40	Unit IA Silty clay	Upper Quaternary	62	30	8		tr	0.6	d	c	d	d	
Hole 485A														
6-3, 11–15	101.11	Unit II	Lower(?) Quaternary	65	26	9			0.7	d	d	d	d	
11-2, 107–111	148.07	Silty clay and turbidites		77	16	7			0.6	d	d	d	d	
11-3, 35–37[a]	158.35			73	21	6			0.6	d	c	d	d	
22-6, 45–48[b]	209.45	Sandy mud, muddy		81	12	7		tr	0.6	c		c	tr	
26-1, 48–50[b]	226.48	nannofossil chalk, and		79	14	7		tr	0.6	c		c	c	
28-1, 148–150[b]	236.48	nannofossil-bearing silty claystone			20	10	50	20		c		c	c	
36-3, 41–49[b]	298.41			83	10	7			0.5	d		c	c	
38-1, 98–100[b]	313.98				20	25		55		d		c	c	c

[a] Sediments just above basement.
[b] Sediments interlayered within basement.
[c] Moderate.
[d] Abundant.
[e] Trace.

Table 12. The b repeat distances of clay minerals and mica poly-
types in sediments, Site 485.

Sample (interval in cm)	Sub-bottom Depth (m)	(b) (Å)	Mica Polytype
Hole 485			
1-2, 90–94	2.40	9.02	
3-4, 120–124	18.20	9.05	
Hole 485A			
1-5, 120–124	52.10	9.02	1M ≫ 2M₁
6-3, 11–15	101.11	9.04 ≥ 9.26	1M ≫ 2M₁
9-1, 128–138	127.78	9.02 ≥ 9.28	1M ≫ 2M₁
11-3, 35–37	158.35	9.04 ≥ 9.20	1M
19-2, 40–42	189.90	9.04 ≥ 9.25	
26-1, 48–50	226.48	9.05 > 9.28	1M ≫ 2M₁
34-1, 33–35	277.33	9.01 ≥ 9.23	
36-2, 58–61	297.08	9.01 ≥ 9.23	1M ≫ 2M₁
38-1, 98–100	313.98	9.00 < 9.25	1M > 2M₁

the authigenic appearance of the clay minerals (Plate 2, Fig. 6).

Mixed-layer chlorite–montmorillonite in samples from Section 484A-38-1 in the dry state has a high, narrow, symmetrical peak at 13.83 Å and a weak low-angle reflection. Other peaks for the mineral are superimposed on chlorite peaks at 7 Å, 4.7 Å, and 3.5 Å. After saturation with glycol, the 13.83 Å peak moves to 15.2–15.4 Å, the 7-Å peak becomes asymmetric, and the low-angle peak becomes sharper. After heating at 550°C, the 13.83 peak moves to 13.4 Å. The mineral is soluble in hot 10% HCl (Table 2) and is trioctahedral in structure with $b = 9.25$ Å (Table 12). The crystal structure of the mineral is similar to that of corrensite. In transmission electron photomicrographs the mineral occurs as elongated plates or needle-like crystals (Plate 1, Figs. 5 and 6). Morphology of the authigenic minerals in samples from Section 38-1 is shown in Plate 3, Figures 1–6. Since the sediments intercalated within basalts contain authigenic chlorite and mica phases, as well as analcime, it is likely that they have undergone hydrothermal alteration.

The coarse fraction (>20 μm) mineralogy was studied by the immersion method in 13 samples from Site 485 (Table 3), 7 of which are from layers in the basement. The heavy fraction content ranges from traces to 1.9 volume percent. It is composed of 44 to 100% pyrite and up to 16% unidentified black opaque minerals; the rest of the heavy minerals are transparent, including up to 13% authigenic barite. Barite occurs only in sediments intercalated within basement. The terrigenous mineral assemblage is similar to that previously described at other sites, but the percentage of transparent minerals in the heavy fraction is higher as a result of lower pyrite content in most samples. The epidote group predominates; hornblende, zircon, and apatite are common; and garnet, clinopyroxene, rutile, anatase, and sphene occur sporadically as rare grains.

The light fraction is composed of quartz, feldspars (mainly sodium plagioclase and potassium feldspar, but with some labradorite also present), and aggregate particles, the latter including clay pellets, rock fragments, and various minerals altered to chlorite or smectite. Zeolite was detected only in the uppermost sample. Gypsum occurs in several samples both above and below the sediment/basement contact.

Geochemistry

Bulk chemical composition was studied in both common hemipelagic mud far above basement and in sediments immediately overlying or within the basement (Tables 13, 14). The composition appeared to be rather monotonous throughout and similar to that at Sites 382 and 384. Silica content and SiO_2 to Al_2O_3 ratios are close to those of average hemipelagic clay or of average shale, both in bulk samples and in clay fractions. The 2–20 μm fraction is somewhat enriched in silica and the SiO_2 to Al_2O_3 ratio ranges from 3.7 to 4.8. The sediments with unusual clay mineralogy from Core 38 are somewhat enriched in silica (the SiO_2 to Al_2O_3 ratio in bulk samples is 3.9).

The titanium content is low, and the Al to Ti ratio ranges both in bulk samples and in the less than 2 μm fraction within the limits of 19 to 27; in several samples it is somewhat higher than that of average clay as a result of the extremely low Ti content. The ratio decreases in the 2–20 μm fraction, as Ti content increases and Al decreases.

The total iron content ranges from 2.8 to 4.2 weight percent in bulk samples, but is commonly higher in the 2–20 μm fraction, ranging up to 6.8% in a sample just above basalt (Sample 485A-11-3, 35–37 cm), where we found abundant ankerite crystals, and up to 5.3% and 4.8%, respectively, in two samples from sediments interlayered within the basement. The clay fraction does not show any noticeable increase in iron, as compared with bulk samples. Fe_2O_3 prevails over FeO both in bulk samples and in each of the size fractions examined, except for the lowermost sample, Sample 485A-38-1, 98–100 cm, where the iron content is low and is represented mostly by FeO[2]. This sample is of unusual clay mineralogy and contains analcime.

We have not found regular downhole changes in any other constituents of the sediments. MgO and CaO variations are rather irregular, although CaO increases sharply (up to 4–6%) in several bulk samples enriched in biogenic $CaCO_3$. The highest value of total alkalinity (as expressed by the ratio of $K_2O + Na_2O$ to Al_2O_3) was found in a previously mentioned sample, 485A-38-1, 98–100 cm, in which the sodium content is also the highest observed. In other samples the total alkalinity values are uniform, the ratio being lowest in the clay fraction as a result of the decrease in sodium and increase in aluminum. The potassium to sodium ratio is more variable, particularly in the clay fraction, where it ranges from 0.8 (in a sample just above basement) up to 6.5 (in sediments with mixed-layer chlorite–montmorillonite), main-

---

[2] Fe in pyrite is included in Fe_2O_3, since it is insoluble in reagents used for FeO determination.

Table 13. Chemical composition of representative sediments, Holes 485 and 485A.

Component	485-1-2, 90–94 cm			485-6-4, 110–114 cm			485A-6-3, 11–15 cm			485A-10-2-104, 107 cm			485A-11-3, 35–37 cm[a]		485A-19-2, 40–42 cm[b]	
	Bulk	2–20 μm	<2 μm	Bulk	2–20 μm	<2 μm	Bulk	2–20 μm	<2 μm	Bulk	2–20 μm	<2 μm	2–20 μm	<2 μm	Bulk	2–20 μm
	52.58	63.96	53.64	54.38	65.02	53.38	57.36	62.08	54.30	55.78	62.60	54.02	56.06	53.50	57.62	56.98
TiO_2	0.49	0.56	0.56	0.55	0.58	0.71	0.62	0.62	0.73	0.58	0.66	0.73	0.66	0.75	0.49	0.71
Al_2O_3	13.94	14.50	16.23	13.88	13.45	17.71	13.90	13.09	17.34	14.80	14.12	17.51	13.64	16.55	13.50	15.57
Fe_2O_3	4.30	3.29	4.46	2.49	3.43	2.66	2.54	2.96	3.83	3.14	3.42	3.25	7.00	6.07	3.81	6.23
FeO	1.12	0.78	1.14	1.36	0.78	1.53	1.84	2.88	1.19	1.36	1.43	1.26	2.45	0.41	0.82	1.16
MnO	0.11	0.07	0.06	0.07	0.08	0.07	0.06	0.08	0.06	0.06	0.07	0.05	0.13	0.05	0.06	0.09
MgO	2.26	1.45	2.42	2.58	1.85	3.06	2.90	2.66	3.38	2.90	2.18	3.06	2.26	2.58	2.98	2.52
CaO	3.02	1.90	0.45	4.48	1.79	0.56	3.58	1.79	1.23	2.69	1.57	1.23	2.46	1.34	6.16	2.24
Na_2O	3.20	2.33	0.94	2.72	2.24	0.62	2.60	2.23	0.67	2.12	2.60	0.5	1.80	3.18	2.60	1.36
K_2O	2.70	3.00	2.31	2.25	2.89	2.00	3.00	3.33	3.00	3.62	2.62	2.62	2.50	2.45	2.62	2.80
P_2O_5	0.08	0.04	0.06	0.19	0.19	0.13	0.21	0.20	0.14	0.13	0.19	0.13	0.16	0.04	0.33	0.07
LOI+	15.8	7.8	17.4	14.5	7.5	17.00	10.8	7.5	13.8	12.4	8.1	15.1	10.3	12.9	8.70	9.7
Total	99.60	99.68	99.79	99.45	99.80	99.43	99.41	99.42	99.67	99.58	99.56	99.46	99.42	99.82	99.69	99.43
K_2O/Na_2O	0.84	1.29	2.46	0.83	1.29	3.22	1.15	1.49	4.48	1.71	1.00	5.24	1.39	0.77	1.00	2.06
$K_2O + Na_2O/Al_2O_3$	0.42	0.37	0.20	0.36	0.38	0.15	0.40	0.42	0.21	0.39	0.37	0.18	0.32	0.34	0.39	0.27
$Fe_2O_3 + FeO + MgO/Al_2O_3$	0.55	0.38	0.49	0.46	0.45	0.41	0.52	0.65	0.48	0.50	0.50	0.43	0.86	0.55	0.56	0.64
SiO_2/Al_2O_3	3.77	4.41	3.30	3.92	4.83	3.01	4.13	4.74	3.13	3.77	4.43	3.08	4.11	3.23	4.27	3.66
Fe	3.88	2.91	4.01	2.80	3.01	3.05	3.21	4.32	3.61	3.26	3.50	3.25	6.81	4.57	3.31	5.26
Al/Ti	25.48	22.59	25.29	22.27	20.37	21.83	19.92	18.76	20.89	22.4	19.18	21.01	18.54	19.49	24.65	19.19

Note: Values shown in weight percent.
[a] Sediments immediately overlying basement.
[b] Sediments intercalated within basalts.

Table 14. Average composition of sediments, Site 485.

Component	Sediments above Basement			Sediments Intercalated within Basalts			Mixed-layer Chlorite-Montmorillonite-bearing Sediments Intercalated within Basalts		
	Bulk ($n = 4$)	2–20 μm ($n = 4$)	<2 μm ($n = 4$)	Bulk	2–20 μm	<2 μm	Bulk	2–20 μm	<2 μm
SiO_2	55.02	63.42	53.84	55.61	60.40	57.30	60.42	64.95	60.54
TiO_2	0.56	0.60	0.68	0.59	0.66	0.62	0.73	0.56	0.73
Al_2O_3	14.13	13.79	17.20	15.20	15.30	16.28	15.53	16.27	17.18
Fe_2O_3	3.12	3.28	3.55	3.47	5.10	3.67	1.93	0.87	2.65
FeO	1.42	1.47	1.28	1.44	1.10	1.23	2.07	1.47	1.74
MnO	0.08	0.08	0.06	0.06	0.08	0.04	0.04	0.03	0.11
MgO	2.66	2.04	2.98	2.68	2.19	2.85	2.82	1.83	3.71
CaO	3.44	1.76	0.87	4.14	1.79	0.82	1.34	0.78	0.45
Na_2O	2.66	2.35	0.68	2.18	1.36	1.20	4.40	3.92	0.58
K_2O	2.89	2.96	2.48	3.04	3.13	3.28	3.44	3.85	3.75
P_2O_5	0.15	0.16	0.14	0.20	0.09	0.16	0.16	0.10	0.28
LOI+	13.38	7.72	15.82	11.02	8.30	12.00	6.90	4.80	7.80
K_2O/Na_2O	1.09	1.26	3.65	1.38	2.30	2.73	0.78	0.98	6.46
$K_2O + Na_2O/Al_2O_3$	0.39	0.38	0.18	0.37	0.29	0.28	0.50	0.48	0.25
$Fe_2O_3 + FeO + MgO/Al_2O_3$	0.51	0.49	0.45	0.50	0.55	0.48	0.44	0.26	0.47

ly as a result of changing sodium content. Phosphorus is low throughout the section studied.

Trace elements were analyzed in 18 samples from Site 485, including 9 samples from sediments intercalated within basalts and 1 from just above basement. Along with bulk samples, we analyzed the clay fraction and the 2–20 μm fraction (Table 15).

The bulk samples show rather insignificant variations in concentrations of trace elements without any increasing (or decreasing) trend in sediments intercalated within basalts. The concentrations and average values are close to those determined at Sites 482 and 484, but Cu, Ni, V, and Zn contents are lower than those at Site 483. Such trace elements as Zn, Cu, Ag, and Sn tend to be concentrated in the 2–20 μm fraction (Table 15). The high concentrations of Zn (up to 995 ppm), Cu (up to 570 ppm), Sn (up to 32 ppm), and Ag (up to 6.5 ppm) in this fraction occur both above and within basement; however, average values apparently show an increasing trend with depth in the latter. The clay fraction (Table 15) is relatively enriched in Cr and V, whereas Zn, Cu, Sn, and Ag are commonly less abundant in this fraction than in the 2–20 μm fraction.

MINERALOGY AND CHEMICAL COMPOSITION OF SEDIMENTS FROM THE MOUTH OF THE GULF OF CALIFORNIA

The Quaternary and upper Pliocene hemipelagic sediments drilled during Leg 65 are composed mainly of terrigenous material—both clay and clastic minerals, derived from nearby mainland Mexico, with minor admixtures of biogenic and authigenic constituents. Composition of the terrigenous material is rather monotonous at all sites throughout the sediment sections drilled. Smectites, represented by aluminous montmorillonite with a dioctahedral structure in which the aluminum is partially replaced by ferric iron, predominate over mica in clay mineral assemblages, while chlorite + kaolinite occur as a minor admixture. Ferric montmorillonite belonging to the Fe-Al-smectite group of Drits and Kossovskaya (1980) is also detected in the sediments, but it is, at least partially, of authigenic origin. The terrigenous smectites show an irregular ''cloudy'' appearance on electron photomicrographs, whereas the authigenic smectites are represented by flat, elongate crystals or by ''honeycomb'' textures.

Table 15. Trace element composition of sediments, Site 485.

Sample (interval in cm)	Sub-bottom Depth (m)	B	Co	Cr	Cu	Mo	Ni	V	Pb	Sn	Zn	Ag	Sc	Zr
Bulk sediments														
Hole 485														
1-2, 90–94	2.40	112	14	50	80	13	91	95	46	3	220	0.37		
4-2, 120–124	24.70	115	13	41	92	91	77	71	40	3	190	0.63		
Hole 485A														
1-5, 120–124	52.10	115	9	53	55	26	68	80	35	4	158	0.27		
3-2, 5–9	71.05	124	9	56	55	17	53	85	46	4	142	0.27		
6-3, 11–15	101.11	107	9	54	55	10	43	92	46	4	138	0.23		
9-1, 128–132	127.78	102	10	54	51	13	44	94	48	4	126	0.23		
10-2, 104–107	138.54	110	10	53	62	14	55	90	46	4	152	0.27		
11-2, 107–111	148.07	78	10	57	46	13	48	91	48	4	126	0.32		
11-3, 35–37[a]	158.35	60	10	54	38	8	39	78	40	4	83	0.27		
19-2, 40–42[a]	189.90	57	11	48	46	11	50	80	44	4	102	0.29		
20-1, 33–35[b]	192.83	93	13	53	60	8	67	94	55	4	200	0.23		
22-6, 45–48[b]	209.45	83	11	53	52	11	50	91	52	5	174	0.33		
26-1, 48–50[b]	226.48	80	11	55	58	21	53	97	48	5	158	0.35		
28-1, 148–150[b]	236.48	60	10	54	55	17	53	80	52	5	148	0.48		
34-1, 33–35[b]	277.33	43	10	44	52	13	55	80	50	4	142	0.37		
36-1, 61–65[b]	295.61	44	8	40	53	14	53	79	42	4	126	0.55		
37-1, 62–65[b]	304.62	62	7	37	46	7	41	83	40	4	166	0.32		
38-1, 98–100[b]	313.98	32	11	50	60	16	53	94	33	4	105	0.37		
Average:														
Sediments overlying basement (n = 8)		108	10	52	62	25	60	87	44	4	156	0.32		
Sediments intercalated within basalts (n = 9)		62	10	48	54	13	53	86	47	4	147	0.37		
Intermediate (2–20 µm) sediment														
Hole 485														
1-2, 90–94	2.40	42	10	30	433	1	52	78	33	7	617	6.3		
4-2, 120–124	24.70	67	17	32	570	121	92	76	81	27	610	6.0		
Hole 485A														
1-5, 120–124	52.10	51	10	43	320	39	70	73	60	12	273	3.8		
3-2, 5–9	71.05	35	7	37	200	10	40	67	40	5	215	2.0		
6-3, 11–15	101.11	36	7	29	138	6	25	65	33	4	190	1.8		
9-1, 128–132	127.78	50	7	32	120	10	32	69	44	4	210	1.3		
10-2, 104–107	138.54	58	8	40	170	13	50	75	52	5	270	1.7		
11-2, 107–111	148.07	58	10	50	155	16	48	89	40	6	260	1.4		
11-3, 35–37[a]	158.35	63	12	50	285	15	57	102	47	10	348	3.4		
19-2, 40–42[b]	189.90	115	20	74	590	17	100	160	96	15	722	5.7		
20-1, 33–35[b]	192.83	63	9	41	230	5	41	93	50	11	303	3.2		
22-6, 45–48[b]	209.45	51	9	33	186	7	37	75	50	9	420	2.3		
26-1, 48–50[b]	226.48	67	11	47	314	10	53	112	69	20	447	2.8		
28-1, 148–150[b]	236.48	82	16	71	400	22	94	155	89	15	518	5.9		
34-1, 33–35[b]	277.33	35	9	41	230	15	50	73	63	10	320	4.4		
36-1, 61–65[b]	295.61	53	4	44	274	5	59	102	65	9	427	3.2		
37-1, 62–65[b]	304.62	71	12	81	515	5	59	123	85	32	995	6.5		
38-1, 98–100[b]	313.98	18	9	32	152	2	38	77	32	9	470	4.0		
Average:														
Sediments overlying basement (n = 8)		50	10	37	263	27	51	74	48	9	331	3.0		
Sediments intercalated within basalts (n = 9)		62	11	52	321	10	59	108	67	14	514	4.2		
Clay <2 µm sediment fraction														
Hole 485														
1-2, 90–94	2.40		12	75	100		48	91	14	—			14	97
4-2, 120–124	24.70	94	24	51	150	18	35	76	13	4	270	2.5	16	150
Hole 485A														
1-5, 120–124	52.10		15	63	118		50	200	17	24			21	135
3-2, 5–9	71.05	170	8	160	210	10	71	190	15	3	270	1.7	22	230
6-3, 11–15	101.11		—	87	112		46	150	18	—			9	170
9-1, 128–132	127.78	120	8	87	90	15	35	180	14	5	300	1.5	14	150
10-2, 104–107	138.54		14	106	130		45	270	10	—			36	270
11-2, 107–111	148.07	130	15	160	160	16	50	190	17	8	400	2.7	30	160
11-3, 35–37[a]	158.35		—	200	88		43	43	15	—			19	130
20-1, 33–35[b]	192.83	80	9	44	105	4	44	100	46	5	248	1.2		
22-6, 45–48[b]	209.45	64	7	39	71	5	30	91	33	4	149	0.89		
26-1, 48–50[b]	226.48	58	9	46	81	13	40	100	52	5	182	0.81		
28-1, 148–150	236.48	59	7	38	86	11	36	103	55	5	172	1.2		
34-1, 33–35[b]	277.33	54	8	54	70	13	54	102	60	6	205	1.2		
36-1, 61–65[b]	295.61	55	9	70	123	8	86	113	47	6	212	1.3		
37-1, 62–65[b]	304.62	98	13	118	233	10	55	207	62	9	327	4.7		
38-1, 98–100[b]	313.98		—	105	74		30	90	6	—			23	100
Average:														
Sediments overlying basement (n = 8)		114	10	99	134	15	48	168	15	6	310	2.1	20	170
Sediments intercalated within basalts (n = 8)		67	9	64	105	9	47	113	45	6	214	1.6		

Note: Values shown in ppm.
[a] Sediments just above basement.
[b] Sediments intercalated within basalts
— = Not detected.

The terrigenous clastic material is composed mainly of quartz and feldspars, the latter represented by sodium plagioclase and potassium feldspar with minor amounts of labradorite. In coarse fractions, quartz and feldspars occur in approximately equal amounts, but commonly the feldspars somewhat predominate, indicating an immature terrigenous mineral assemblage. The transparent heavy mineral fraction is represented by an epidote–hornblende–zircon–apatite assemblage in which epidote strongly predominates. This assemblage is typical of the sediments associated with the circum-Pacific Mesozoic–Cenozoic orogenic belt.

Biogenic constituents occur in minor amounts. Biogenic opal (diatoms, radiolarians, and sponge spicules) is common in the upper portions of sediment sections at all sites. It becomes rare below 50 meters and disappears below 100 meters at Site 482 (upper Quaternary); becomes rare below 70 meters and disappears below 90 meters at Site 483 (lower Quaternary); becomes rare below 50 meters at Site 484 (upper Quaternary); becomes rare below 50 meters and virtually disappears below 90 meters at Site 485 (lower Quaternary). Just above the complete disappearance level, we observed partly dissolved forms. The dissolution features together with the different stratigraphic positions of the disappearance level provide evidence of diagenetic dissolution of the biogenic opal, likely stimulated by heating of the sediment column from below. The distribution of biogenic carbonates, on the other hand, is rather irregular, likely reflecting differences in primary sedimentation.

Along with terrigenous and biogenic minerals we identified several authigenic constituents. Some of the authigenic minerals (pyrite, carbonates) show distribution patterns that are independent of sub-bottom depth or proximity to basalt, whereas others, such as barite, mixed-layer chlorite–montmorillonite and illite–montmorillonite ($\pm$ mica), swelling chlorite, ferric montmorillonite, analcime, and gypsum, occur mainly (or solely) in sediments close to the sediment/basement contact or intercalated within basement, thus likely being related either to hydrothermal activity or to heating by hot basalt. We found two layers within basement at Site 485 in which clay minerals are represented mainly by authigenic mixed-layer phases with analcime, and a layer at Site 482 which is entirely composed of authigenic (hydrothermal) illite–montmorillonite ($+$ mica) and swelling chlorite. One sample from Hole 482, about 7 meters above the basalt contained dolomite–ankerite. Clinoptilolite is absent from zones of possible hydrothermal influence, occurring only in the upper parts of sediment sections.

The bulk chemical composition of sediments from the mouth of the Gulf is similar to that of common hemipelagic terrigenous clay and silty clay found elsewhere (e.g., Goldberg and Arrhenius, 1958; Landergreen, 1964; Mikhailov, 1980; Kurnosov et al., in press; Murdmaa et al., 1979, 1980). As compared with the Miocene hemipelagic clay in the western North Atlantic (Murdmaa et al., 1979), which is also mainly smectitic, the sediments considered here contain less aluminum, titanium, and iron, but more alkali metals and calcium,

the latter associated in part with biogenic carbonate. They differ from Japan trench hemipelagic sediments (Murdmaa et al., 1980) in having a lower silica content as a result of the scarcity of siliceous microfossils, but the interrelations between other constituents are similar.

We compared the bulk chemistry of the sediments from the mouth of the Gulf of California with that of continental arkoses and graywackes (Middleton, 1960; Baily et al., 1964; Ronov et al., 1965; Schwab, 1971; Crook, 1974; Shutov, 1975) and found that percentages of most constituents, as well as the values of the K_2O/Na_2O, $K_2O + Na_2O/Al_2O_3$, and $Fe_2O_3 + FeO + MgO/Al_2O_3$ ratios, resemble those obtained in argillaceous members of the upper Cretaceous to Miocene flysch deposits in the eastern Kamchatka (Markevich, Chudaev, 1979).

The composition of the various size fractions examined often differs markedly from that of bulk samples, showing different contributions of clay, clastic minerals, and biogenic constituents to the total sediment chemistry. The 2–20 μm fraction is generally enriched in silica ($SiO_2/Al_2O_3 > +4$) compared with bulk samples and with the clay fraction due to the presence of clastic quartz and partially to biogenic opal. Titanium and aluminum, on the contrary, are higher in the clay fraction, as these elements are associated with clay minerals.

The behavior of iron is more complicated, because it occurs in many minerals of different origin, such as smectites, authigenic pyrite, ankerite, free hydrated oxides, and a wide variety of clastic minerals. As a result, total iron is sometimes greatest in the 2–20 μm fraction and sometimes in the clay fraction. A significant increase in iron (more than 5%) was found in the 2–20 μm fraction from Hole 485A, Cores 11 and 19, both just above basalts. Sample 485A-11-3, 35–37 cm contains in a smear slide abundant ankerite(?) crystals, and Sample 485A-19-2, 40–42 cm is enriched in pyrite. The samples with unusual clay mineralogy (mixed-layer clay minerals or illite–montmorillonite plus mica) at Sites 482 and 485 do not show a regular change in total iron with depth in any fraction, but FeO is more abundant in these samples than is Fe_2O_3. However, oxidation states (i.e., Fe_2O_3/FeO) inferred from the analyses presented here are unreliable, because the iron in pyrite is included in the values shown for Fe_2O_3. So the increase in total iron and Fe_2O_3 in several samples of the 2–20 μm fraction is likely on account of pyrite, as the pyrite spherules and crystals fall mainly in this size range.

Manganese content is low throughout the set of samples analyzed, indicating early diagenetic removal of the element under reducing conditions.

Magnesium is relatively concentrated in the clay fraction, being associated with clay minerals. Calcium, on the contrary, is higher in coarse fractions, following the distribution of biogenic calcite.

Total alkalinity ($K_2O + Na_2O/Al_2O_3$) appeared to be higher in the 2–20 μm fraction than in the clay fraction mainly because of higher sodium and lower aluminum percentages. The potassium to sodium ratio markedly increases in the clay fraction, as sodium decreases. This is consistent with sodium being associated mainly with

plagioclase and clinoptilolite and potassium being incorporated within clay minerals, in both smectites (Fe–montmorillonite) and mica.

Trace elements show the concentration range typical for reduced hemipelagic sediments. Zinc in bulk samples strongly prevails over other elements (more than 100 ppm and up to 440 ppm). The next most abundant elements are V, B, Ni, and Cu (characteristic values 50–100 ppm). The third group comprises Cr and Pb (commonly 30–60 ppm). Molybdenum concentration is generally lower, but shows wide variations (7–91 ppm, with common values ranging within 10–30 ppm). Cobalt content (7–18 ppm) is commonly lower than that of molybdenum. Tin concentration (2–4 ppm) is close to the level of detection, and silver (0.19–0.55 ppm) is only marginally detectable.

Such trace elements as Zn, Cu, Sn, and Ag, and to a smaller extent, Co and Ni tend to have higher concentrations in the 2–20 μm fraction as compared with bulk samples. This probably reflects the presence of authigenic pyrite in the 2–20 μm fraction. Chromium, vanadium, and boron all tend to concentrate in the clay fraction.

Comparing the trace elements at different sites we found that sediments are richest in Zn, Cu, Ni, Co, and V in both bulk samples and individual size fractions at Site 483. At other sites similar high values occur in the 2–20 μm fraction of sediments intercalated within basalts or just above basement. The spectral analysis data, however, should be used with care because some of the concentrations observed in size fractions contradict those in bulk samples (particularly in the case of silver).

HYDROTHERMAL ALTERATION OF SEDIMENTS

One of the objectives of this study was to determine the effects of hydrothermal activity and high heat flow on the sediment composition in the vicinity of a young active rift system. Throughout this study, the sediments immediately overlying basement and those intercalated within basement have been distinguished from the sediment section far above basement in order to discern such effects. However, in most cases we failed to find regular changes which might be attributed to alteration under high temperature or extensive infiltration of juvenile hydrothermal solutions. Nevertheless the sediments display some unusual features, which may be best explained as the result of weak thermal alteration.

As we noted above, the upper Quaternary sediments at all sites contain clinoptilolite, which disappears downhole with increasing temperature. Such young clinoptilolite-bearing sediments are uncommon themselves, but even more unusual is the disappearance of clinoptilolite at sub-bottom depths of about 110 to 160 meters near basement. Siliceous biogenic particles disappear somewhat higher in the section, probably as a result of dissolution under conditions of increased temperature.

The heating of sediments possibly stimulates formation of such authigenic minerals as barite, gypsum, and carbonates of the dolomite–ankerite group. The appearance of these minerals in thin sections (spherulitic and

poikiloblastic textures, euhedral crystals with sediment inclusions) suggests that they formed *in situ*. Although these authigenic minerals occur throughout the section, we noted an increase in their frequency near and within basement, where temperatures must have been higher. Radiating spherulites of barite, for example, were found only in the lower part of the sediment section (beginning about 27 m above the basement) at Site 482 and in sediments intercalated within basement at Sites 482, 483, and 485. Similarly, poikiloblastic carbonate (dolomite?) micronodules occur in two lowermost sediment samples at Site 485 (those composed of authigenic mixed-layer clay minerals and analcime), and dolomite–ankerite crystals are common near the sediment/basement contact and within the basement in Hole 482C. As suggested by Hein et al. (1979) from studies of sediments in the Bering Sea, such carbonates may well be of hydrothermal origin.

We hesitate to include pyrite among the hydrothermal minerals, because unlike barite, gypsum, and ankerite, it is a common early diagenetic mineral in reduced hemipelagic sediments elsewhere. However, any additional iron of hydrothermal origin is likely to be bound up in pyrite, and some sediments rich in pyrite within the basement may have been affected by such activity near the ridge crest.

The high heat flow observed at the Leg 65 sites probably results in alteration of primary terrigenous clay minerals or leads to the formation of new ones. We noted authigenic crystallographic forms of ferric montmorillonite (ribbon-like crystals) (Kossovskaya, 1975) near the sediment/basalt contacts and detected authigenic (probably hydrothermal) mixed-layer clay minerals in several beds at the sediment/basalt contact or intercalated within basalts. The authigenic minerals predominate in the clay mineral assemblages in these beds or compose them entirely and consist of mixed-layer illite–montmorillonite (+mica) together with swelling chlorite at Site 482 and mixed-layer mica–montmorillonite together with chlorite-montmorillonite at Site 485. In Core 485A-38 the mixed-layer clay minerals are associated with analcime, likely of hydrothermal origin. The downhole increase in ferric montmorillonite may be attributed to a low-temperature hydrothermal process as well.

Changes in bulk chemistry of sediments near the sediment/basalt contact and within the basement are rather insignificant. We have not noted any regular increase in iron or manganese in these layers, except for a sample just above basement at Site 485, where iron content in the 2–20 μm fraction is 6.8%. Thus, true metalliferous sediments are absent, in spite of high heat flow and the previously mentioned mineralogical evidence of hydrothermal activity.

However, the layers with unusual authigenic clay minerals differ somewhat chemically from common hemipelagic sediments. Those with illite–montmorillonite (+mica) and swelling chlorite at Site 482 show an increase in Al_2O_3, FeO, and MgO contents and in the K_2O to Na_2O ratio in the clay fraction. Those with hydrothermal mixed-layer mica–montmorillonite and chlorite-

montmorillonite from Core 485A-38 are somewhat enriched in silica, but poor in iron (especially in Fe_2O_3). At the same time, the clay fraction in this material displays the highest potassium to sodium ratio, while the coarser fractions are relatively enriched in sodium.

The variations in trace elements seem to be independent of their distance from basalts, and their concentration in sediments just above or within basement does not increase regularly with depth as might be expected if they were related to hydrothermal activity. The average values show an increase in Zn, Cu, Pb, and Ag in the 2–20 μm fraction from sediments intercalated within basement at Sites 482 and 485, but none in the bulk samples. The maximum concentrations of most trace elements occur together both above and within basement. The samples with unusual, probably hydrothermal, mineralogy are rather poor in trace elements.

It should be emphasized that none of the trace elements studied occurs in concentrations markedly exceeding the limits characteristic for common hemipelagic sediments. Some relatively high values of zinc and copper occur among the bulk samples analyzed, particularly in the lower portions of sediment sections, but they show little relation to the basalts. These concentrations may be related to hydrothermal activity, but more likely are associated with authigenic iron sulfides derived from interstitial waters. The high concentrations of both trace elements and pyrite in the 2–20 μm fraction confirms the assumption.

In any case, we have not found high concentrations of the trace elements like those in metalliferous sediments from the Red Sea or the East Pacific Rise. Any hydrothermal activity in the vicinity of the sites was thus too weak or distant to overcome either dilution in the voluminous terrigenous sediments deposited in the area or migration of the elements under the strongly reducing conditions which prevailed during early diagenesis.

CONCLUSIONS

Adjacent to an active spreading center in the Gulf of California, terrigenous hemipelagic sediments are rapidly accumulating, composed of clay minerals (with Al- or Al–Fe–smectite as the dominant constituent), quartz, and feldspars. The minor components of the sediments are terrigenous heavy minerals, biogenic silica, and calcium carbonate and authigenic clinoptilolite, pyrite, ferric montmorillonite, mixed-layer clay minerals, and carbonates of dolomite–ankerite group. Barite and gypsum occur in trace amounts.

Notwithstanding the high thermal gradients and heat flow in the region, we found only minor geochemical or mineralogic evidence of hydrothermal alteration of the sediments even in beds just above basement or in those intercalated within basalts. This is consistent with the fact that the basalts, for the most part, are only slightly altered. The basalts are generally massive, well crystallized, relatively unfractured, and only slightly vesicular, which suggests that the magmas were relatively dry and contained only limited amounts of volatiles. Therefore, the volcanism commonly associated with rather weak hydrothermal activity and extensive infiltration of juvenile hydrothermal solutions into the sediment column has not taken place.

The observed changes in mineral composition of the terrigenous sediments, such as authigenic clay mineral formation (ferric montmorillonite in flat, elongate crystals, mixed-layer chlorite-montmorillonite, mica–montmorillonite ± mica, and swelling chlorite), precipitation of barite, gypsum, dolomite–ankerite, and analcime, as well as downhole dissolution of siliceous microfossils and the disappearance of clinoptilolite, are likely caused by heating of the water-saturated sediments, rather than by the infiltration of hydrothermal solutions into the sediments or the interaction of such solutions with bottom waters.

The previously mentioned authigenic minerals do not result in significant changes in total chemical composition of the terrigenous hemipelagic sediments studied. The mobile forms of iron are precipitated during early diagenetic breakdown of organic matter under reducing conditions as authigenic pyrite, and partially as ankerite, the latter being likely stimulated by increased temperature. We have not found any chemical evidence of metalliferous sediments either in major or in trace elements. The chemical properties of sediments above and within basement vary within limits characteristic of common terrigenous hemipelagic sediments. The very high sedimentation rates in the region may result in dilution of metals derived from the hydrothermal sources commonly associated with active spreading centers.

REFERENCES

Bailey, E. H., Yrwin, W. P., and Jones, D. L., 1964. Franciscan and related rocks, and their significance in the geology of Western California. *Bull. Calif. Div. Mines Geol.*, 183:3–171.

Biscaye, P. E., 1964. Mineralogy and sedimentation of the deep-sea sediment fine fraction in the Atlantic Ocean. *Geochem. Tech. Rept.*, 8:803.

Crook, K. A., 1974. Lithogenesis and geotectonics: The significance of compositional variation in flysch arenites (graywackes). *Modern and Ancient Geosynclinal Sedimentation*: (Tulsa, Okla. Proc. Sym. Madison, Wisc.), 74:304–309.

Drits, V. A., and Kossovskaja, A. G., 1980. Geocrystallochemistry of rock-forming diactohedral smectites. *Lithol. Miner. Resour.*, 1: 84–114.

Goldberg, D., and Arrenius, G. O., 1958. Chemistry of Pacific pelagic sediments. *Geochim. Cosmochim. Acta*, 13:1134–1159.

Hein, J. R., O'Nell, J. R., and Jones, M. G., 1979. Origin of authigenic carbonates in sediment from the deep-Bering Sea. *Sedimentology*, 26:681–705.

Kossovskaya, A. G., 1975. Geocrystallochemistry in the solution of geological problems. *Crystallochemistry of Minerals and Geological Problems*: Moscow (Nauka), pp. 7–18.

Kurnosov, V. B., Mikhailov, M. A., and Shevchenko, A. Ya., in press. Mineralogy and geochemistry of sediments and secondary alteration products of basalts of the Bering Sea and northern Pacific. *Geology of the Bering Sea*: Vladivostok.

Landergreen, S., 1964. On the geochemistry of deep-sea sediments. *Bull. Calif. Div. Mines Geol.*, 10:57–79.

Markevich, P. V., and Chudaev, O. V., 1979. On the composition of sandstones from flysch formations of the Sikhote Alin and Kam-

chatka. *Geochemistry and Mineralogy of Sedimentary Complexes of the Soviet Far East:* Vladivostok, pp. 3–20.

Middleton, G., 1960. Chemical composition of sandstones. *Geol. Soc. Am. Bull.*, Vol. 7.

Mikhailov, M. A., 1980. Petrochemistry and geochemistry of sediments from Komandorskaja basin. *Geology of Komandorskaja Basin:* Vladivostok, pp. 47–63.

Murdmaa, I. O., Gordeev, V. V., Emelyanov, E. M., et al., 1979. Inorganic geochemistry of Leg 43 sediments. *In* Tucholke, B. E., Vogt, P. R., et al., *Init. Repts. DSDP*, 43: Washington (U.S. Govt. Printing Office), 675–694.

Murdmaa, I. O., Gordeev, V. V., Kuzmina T. N., et al., 1980. Geochemistry of the Japan Trench sediments. *In* Scientific Party, et al. *Init. Repts. DSDP*, 56–57, Pt. 2: Washington (U.S. Govt. Printing Office), 1213–1232.

Ronov, A. B., Girin, Yu. P., Kazakov, G. A., et al., 1965. Comparative geochemistry of geosynclinal and platform sedimentary units. *Geokhim*, 8:137–162.

Schutov, V. D., 1975. *Mineral Paragenesis of Graywacke Complexes:* Moscow (Nauka).

Schwab, F. L., 1971. Geosynclinal composition and the new global tectonics. *J. Sed. Petrol.*, 71(4):191–208.
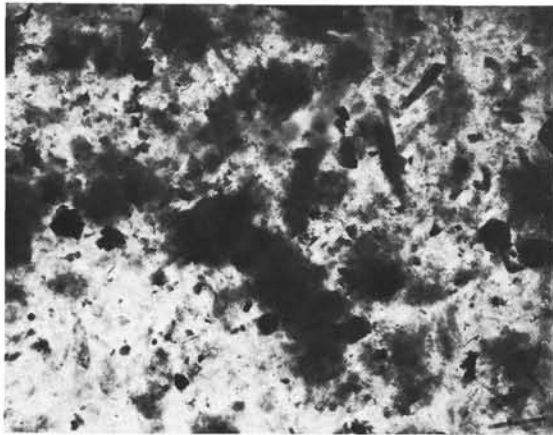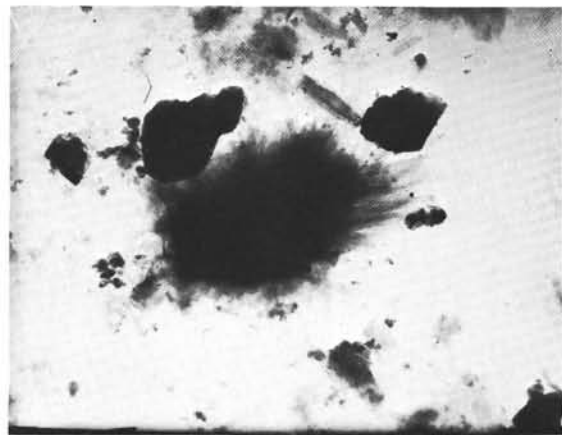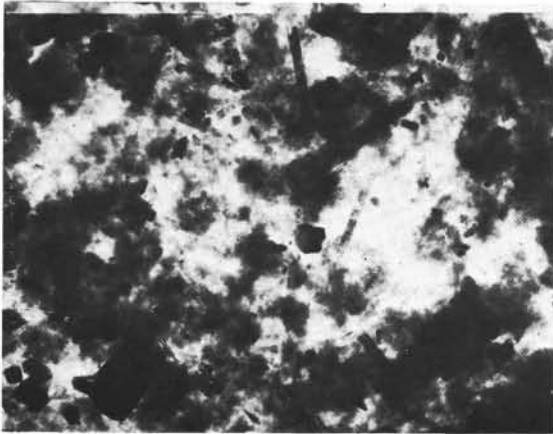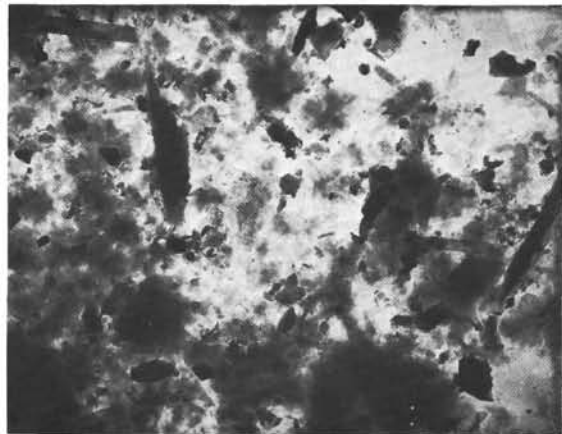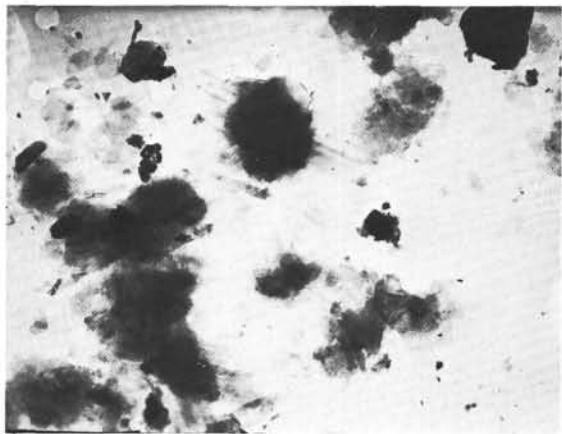
Plate 1. Electron microscope photographs of clay minerals in sediments from the mouth of the Gulf of California. 1, 2. Smectites, Sample 482B-10-7, 4–6 cm, (1) ×12,000, (2) ×18,000. 3. Mixed-layer hydromica–montmorillonite, Sample 482D-9-1, 3–7 cm, ×10,000. 4, 5, 6. Mixed-layer clay minerals, (4) Sample 485A-28-1, 148–150 cm, ×12,000, (5) Sample 485A-38-1, 98–100 cm, ×12,000, (6) Sample 485A-38-1, 98–100 cm, ×12,000.
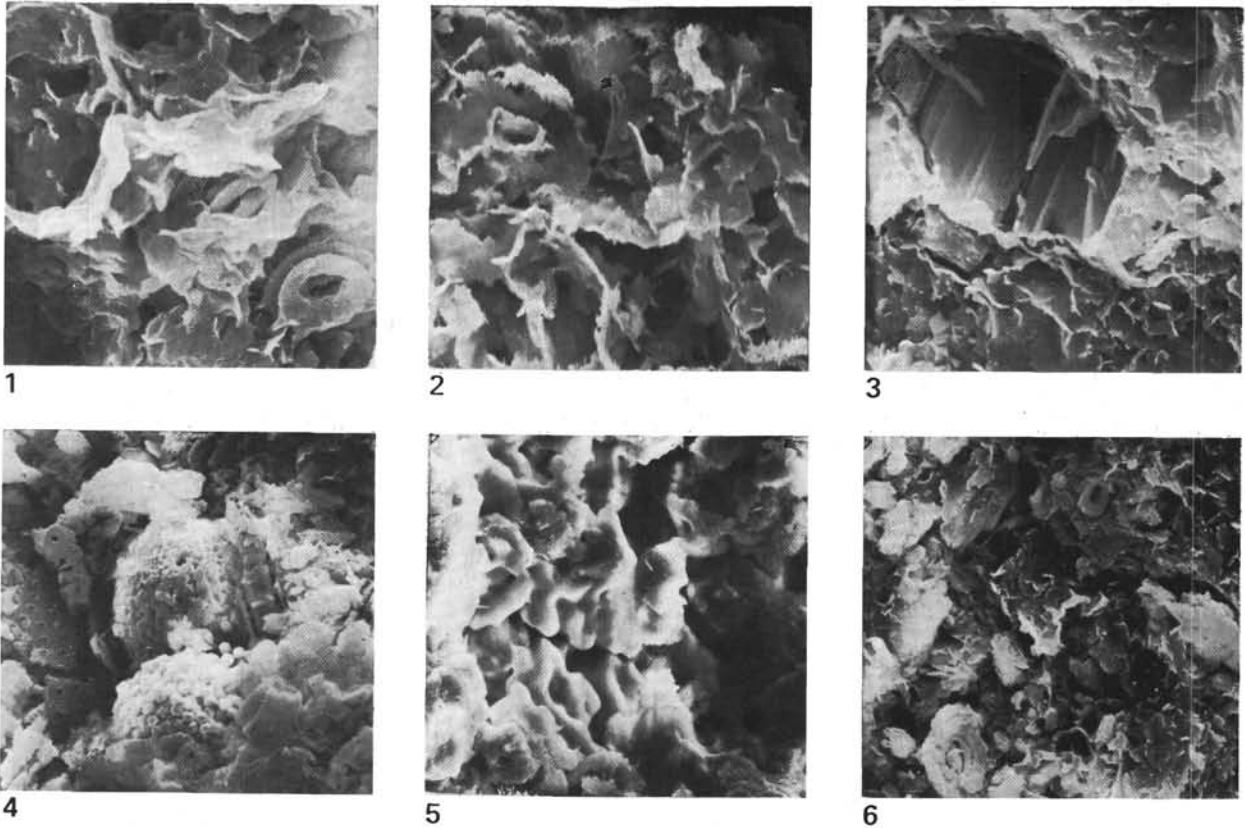
Plate 2. Scanning electron microscope photographs of sediments from the mouth of the Gulf of California. 1. Authigenic smectite and coccoliths, ×1,500, Sample 482D-5-2, 60–63 cm. 2. Mixed-layer illite–montmorillonite (+ mica), Sample 482D-9-1, 5–7 cm, ×1500. 3. Zeolites, ×1,500, Sample 482D-9-1, 5–7 cm. 4. Diatoms, pyrite, and smectite, ×450, Sample 485-1-2, 90–94 cm. 5. Sintered(?) crust of authigenic clay minerals, ×250, Sample 485A-11-3, 35–37 cm. 6. Mixed-layer clay minerals and coccoliths, ×750, Sample 485A-28-1, 148–150 cm.
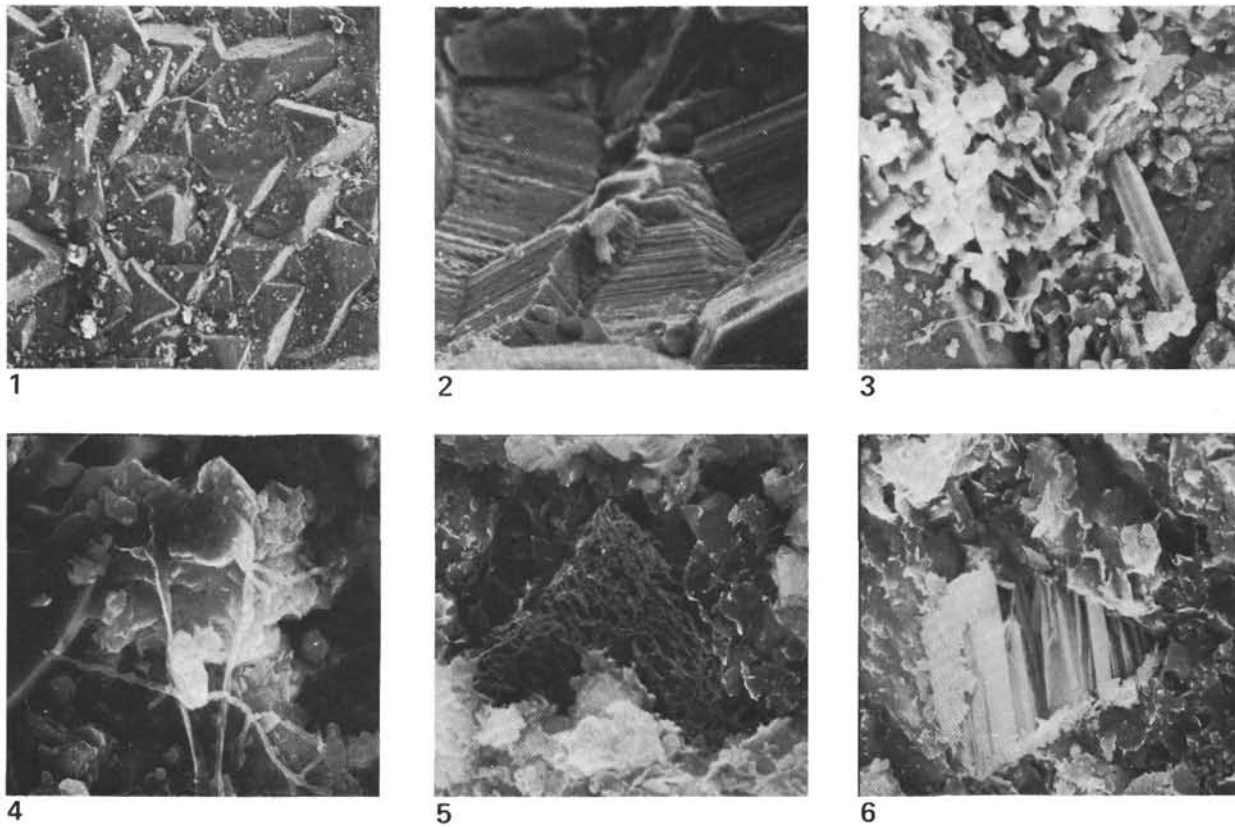
Plate 3. Scanning electron microscope photographs of secondary minerals in sediments from the mouth of the Gulf of California, Leg 65. 1–4. Authigenic vein minerals, Sample 485A-38-1, 94–96 cm, (1) pyrite, ×25, (2) pyrite, ×250, (3) ×150, (4) ×500. 5, 6. Authigenic minerals in sediments, Sample 485A-38-1, 94–96 cm, (5) ×750, (6) zeolites and clay minerals, ×750.